Journal of Medicinal Chemistry

Article

Discovery of (R)-2-(6-methoxynaphthalen-2-yl)butanoic acid As a Potent and Selective Aldo-keto Reductase 1C3 Inhibitor

Adegoke O. Adeniji, Md. Jashim Uddin, Tianzhu Zang, Daniel Tamae, Phumvadee Wangtrakuldee, Lawrence J. Marnett, and Trevor M. Penning

J. Med. Chem., **Just Accepted Manuscript** • DOI: 10.1021/acs.jmedchem.6b00160 • Publication Date (Web): 03 Aug 2016

ACS Publications

Journal of Medicinal Chemistry is published by the American Chemical Society. 1155 Sixteenth Street N.W., Washington, DC 20036

Discovery of (*R*)-2-(6-methoxynaphthalen-2-yl)butanoic acid As a Potent and Selective Aldo-keto Reductase 1C3 Inhibitor.

Adegoke Adeniji; [1] *Md Jashim Uddin*[2] *Tianzhu Zang*[1] *Daniel Tamae;*[1] *Phumvadee Wangtrakuldee*[1]*, Lawrence J Marnett;* [2*] *Trevor M Penning.*[1*]

[1]Department of Systems Pharmacology and Translational Therapeutics and the Center for Excellence in Environmental Toxicology, Perelman School of Medicine, University of Pennsylvania, 1315 BRBII/III, 421 Curie Blvd, Philadelphia, PA 19104-6160

[2]Departments of Biochemistry, Chemistry, and Pharmacology, Vanderbilt Institute of Chemical Biology, Center in Molecular Toxicology, Vanderbilt-Ingram Cancer Center, Vanderbilt University School of Medicine, Nashville, Tennessee 37232-0146, United States

(150 word limit)

ABSTRACT: Type 5 17β-hydroxysteroid dehydrogenase, aldo-keto reductase 1C3 (AKR1C3) converts Δ^4-androstene-3,17-dione and 5α-androstane-3,17-dione to testosterone (T) and 5α-dihydrotestosterone, respectively in castration resistant prostate cancer (CRPC). In CRPC, AKR1C3 is implicated in drug resistance, and enzalutamide drug resistance can be surmounted by indomethacin a potent inhibitor of AKR1C3. We examined a series of naproxen analogs and find that (*R*)-2-(6-methoxynaphthalen-2-yl)butanoic acid (in which the methyl group of *R*-naproxen was replaced by an ethyl group) acts a potent AKR1C3 inhibitor that displays selectivity for AKR1C3 over other AKR1C enzymes. This compound was devoid of inhibitory activity on COX isozymes and blocked AKR1C3 mediated production of T and induction of PSA in LNCaP-AKR1C3 cells as a model of a CRPC cell line. *R*-Profens are substrate selective COX-2 inhibitors and block the oxygenation of endocannabinoids, and in the context of advanced prostate cancer *R*-profens could inhibit intratumoral androgen synthesis and act as analgesics for metastatic disease.

INTRODUCTION

The development of castrate resistant prostate cancer (CRPC) in patients that have undergone androgen deprivation therapy (ADT) is driven by reactivation of androgen receptor (AR) signaling within the tumor in the presence of castrate levels of circulating androgens.[1, 2] AR reactivation results from adaptive intratumoral androgen biosynthesis[3-5] and from changes in the AR itself, including gene amplification[6], AR mutations that make the receptor ligand permissive [7 8], and the appearance of AR splice variants [9, 10] which make the receptor constitutively active.

The importance of the conversion of adrenal androgens into testosterone (T) and 5α-dihydrotestosterone (5α-DHT) or *de novo* androgen biosynthesis within the tumor is firmly established by the therapeutic efficacy of Abiraterone acetate (AA); an inhibitor of P450c17 (17α-hydroxylase/17,20 lyase) in CRPC patients.[11-15] However, concerns over the need for co-administration of prednisone with AA to prevent adrenal insufficiency and the rapid appearance of drug resistance indicates a pressing need for new therapeutic agents. [16, 17]

Aldo-keto reductase 1C3 (AKR1C3) also known as type 5, 17β-hydroxysteroid dehydrogenase (HSD17B5), is a 17-ketoreductase that catalyzes the NADPH dependent conversion of androgen precursors, 4-androstene-3,17-dione (Δ^4–AD) and 5α-androstan-3,17-dione (5-Adione) to yield the potent androgens, T and 5α-DHT, respectively (Scheme 1).[18, 19] AKR1C3 also catalyzes the conversion of androsterone to 5α-androstane-3α,17β-diol the precursor of 5α-DHT in the backdoor pathway.[20, 21] AKR1C3 is one of the most highly over expressed steroidogenic enzymes in CRPC compared to

normal prostate tissue and prostate cancer.[22-26] Moreover, it is dramatically upregulated by ADT. [23, 27, 28] Upon ADT, AKR1C3 is induced by the TMPRSS2-ERG fusion protein, whereby the ERG transcription factor can override the repressive effects of the AR binding to the AKR1C3 promoter. [29] AKR1C3 also plays a role in resistance to P450c17 inhibition by AA observed in prostate cancer cell lines and xenografts [16, 17] AKR1C3 may also act as an AR selective coactivator that promotes tumor growth and this coactivator function could be blocked with small molecule enzyme competitive inhibitors. [30]

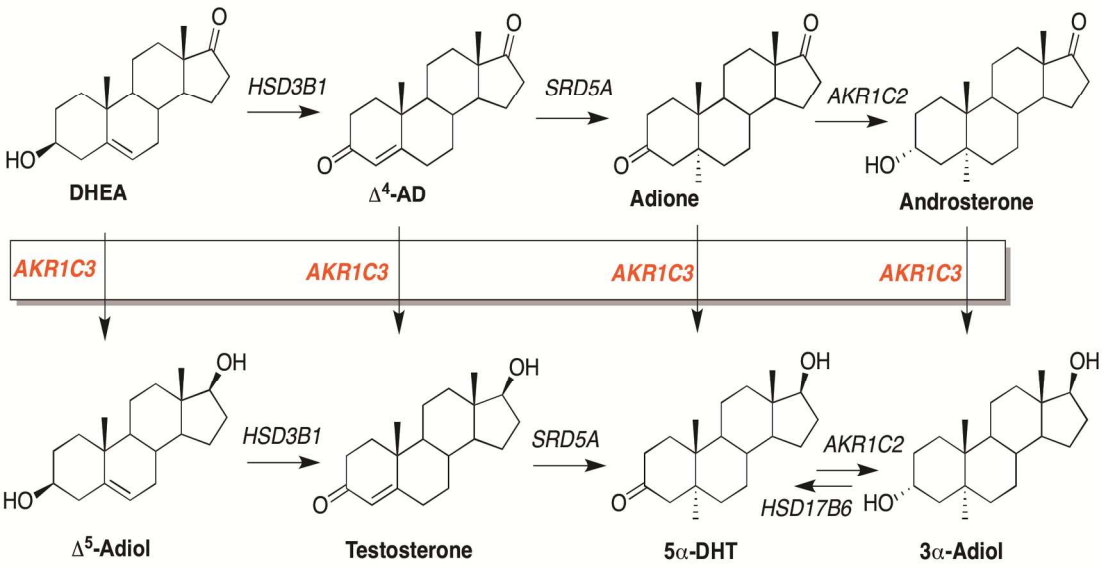

Scheme 1. Central role of AKR1C3 in androgen biosynthesis in prostate cancer. DHEA = dehydroepiandrosterone; Δ^4-AD = Δ^4-androstene-3,17-dione; Adione= 5α-androstane-3,17-dione; Δ^5-Adiol = Δ^5-androstene-3β,17β-diol; 5α-DHT = 5α-dihydrotestosterone; enzymes are referred to by their gene names and are italicized: *HSD3B1* = 3β-hydroxysteroid dehydrogenase type 1; *SRD5A* 5α-reductase type 1 or type 2; *AKR1C2* = type 3 3α-hydroxysteroid dehydrogenase; and *HSD17B6* = 17β-hydroxysteroid dehydrogenase type 6.

Enzalutamide (ENZ) is an AR super-antagonist which is also used to treat CRPC patients, [31-33] and drug resistance also occurs with this agent. ENZ drug resistance in cell lines and in xenografts could be surmounted with indomethacin a non-steroidal antiinflammatory drug (NSAID) and competitive inhibitor of AKR1C3 identified in this laboratory.[34, 35] We are repurposing NSAIDs to be devoid of COX-1 or COX-2 inhibition while maintaining their inhibitory potency for AKR1C3. We have previously reported on indomethacin and fenamate analogs that have the requisite nanomolar inhibitory potency and selectivity for AKR1C3.[36,37] These agents do not inhibit COX-isozymes, nor do they inhibit AKR1C1 and AKR1C2, which are required for the inactivation of 5α-DHT within the prostate.[38-40]

Naproxen, (*S*)-2-(6-methoxynaphthalen-2-yl)propanoic acid is a NSAID that is used clinically to block cyclooxygenase (COX) mediated inflammation. It is also a potent AKR1C3 inhibitor that inhibits the AKR1C3 catalyzed reduction of the bioreductive drug PR-104 in multiple human cancer cells lines and a lung cancer xenograft model.[41] However, naproxen also inhibits AKR1C2 [34] which limits its therapeutic potential in CRPC.

We set out to develop naproxen based AKR1C3 inhibitors that would be useful in CRPC but are devoid of inhibitory activity on COX and other AKR1C enzymes. We report the discovery of (*R*)-2-(6-methoxynaphthalen-2-yl)butanoic acid as a competitive, potent and selective AKR1C3 inhibitor which identifies *R*-profens as a new class of repurposed NSAIDs for CRPC patients. *R*-profens are also substrate selective inhibitors of COX-2 oxygenation of endocannabinoids raising the prospect that in the context of

prostate cancer they may prevent intratumoral androgen biosynthesis and act as analgesics in metastatic disease. [42,43]

RESULTS

Chemistry

S-Naproxen **1** was the precursor of compounds **5, 6** and **9-11** (Schemes 2 and 3). A common intermediate was *S*-methyl-2-(6-trifluoromethylsulfonyloxynaphthalene propanoate, **4** This compound was synthesized from *S*-naproxen which was converted to *O*-demethyl naproxen **2** under acidic conditions followed by esterification to yield, **3**.[42] Subsequent addition of trifluoromethane sulfonic anhydride in base gave **4**. Compound **4** was converted to compound **5** via the 6-vinylogous intermediate and deesterification. The protected acid **3** was converted to the ethoxy intermediate using iodoethane and desesterification gave compound **6** (Scheme 2). Coupling of **4** with sodium triisopropylsilanethiolate followed by deprotection with tetrabutylammonium fluoride gave (*S*)-2-(6-(methylthio)naphthalen-2-yl)propanoate **8**, which upon base hydrolysis yielded the racemic acid, 9. The racemic acid was further oxidized with *m*-chloroperoxybenzoic acid to yield racemic 2-(6-methylsulfinyl)naphthalene-2-yl)propanoic acid **10**, Scheme 3. The steps to compound **11** are identical except the final oxidation of the methyl-thio derivative to yield the methylsufonyl derivative used potassium peroxymonosulfate (Oxone), Scheme 3. Compound **14** was synthesized in two steps from 2-bromo-6-methoxy-naphthalene **12**.[42] Compound **15** was synthesized from racemic 14 via 1,1'-carbonyldiimidazole coupling of methanesulfonamide, Scheme 3.

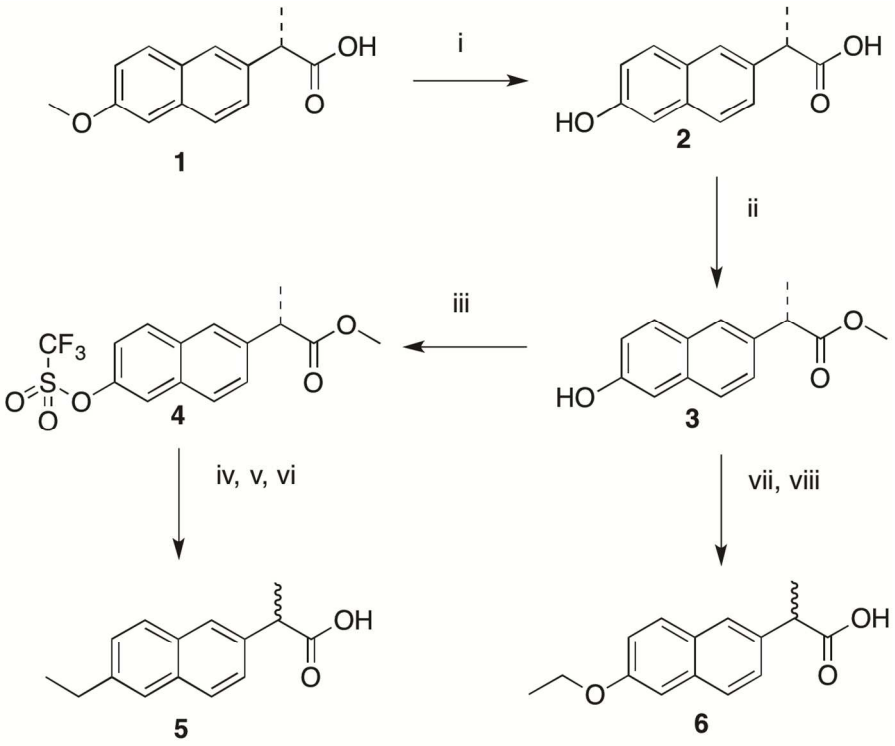

Scheme 2. Synthesis of racemic naproxen analogs **2** and **3**[a] [a]Reagents and conditions: (i) 48% HBr, AcOH, reflux, 3h; (ii) TMSCl, CH_3OH, 25 °C, 2 h; (iii) $(CF_3SO_2)_2O$, Et_3N, DCM, 25 °C, 1 h; (iv) CH_2=$CHBF_3K$, Cs_2CO_3, $Pd(PPh_3)_4$, Et_3N, EtOH, 50 °C, 16 h; (v) $(OAc)_2Pd$, *t*-But_3P, HCO_2H, 25 °C, 12 h; (vi) 3M KOH/CH_3OH, reflux, 3h, (vii) KOH,C_2H_5I, 25 °C, 30 min; (viii) 3M KOH/ CH_3OH, reflux, 2 h.

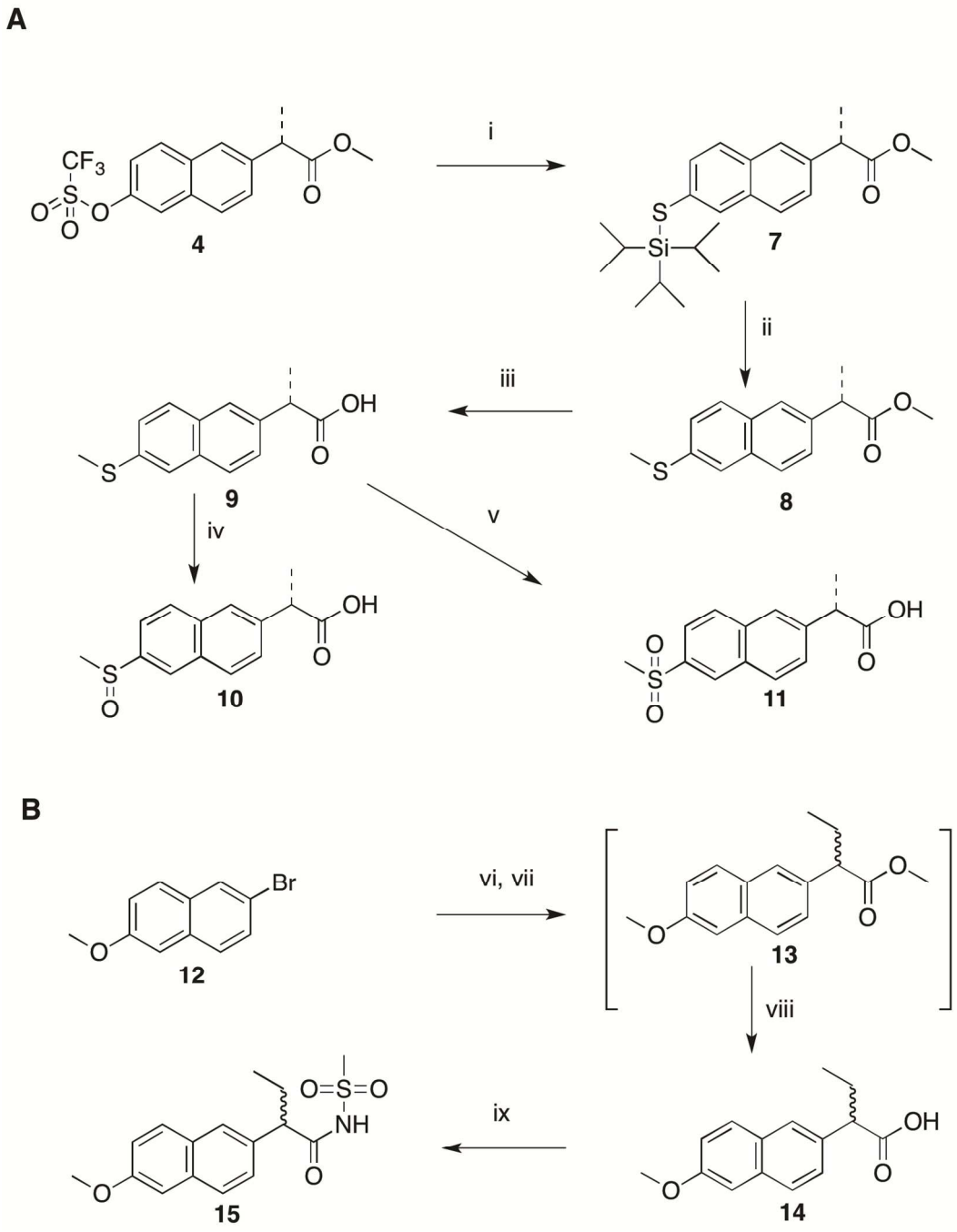

Scheme 3. Synthesis of racemic naproxen analogs . Reagents and conditions: (i) $Pd(PPh_3)_4$, $[(CH_3)_2CH]_3SiSH$, C_6H_6, reflux, 4 h; (ii) TBAF, CH_3I, 25 ^oC, 2 h; (iii) 3M KOH/ CH_3OH, reflux, 2h; (iv) mCPBA, DCM 0 ^oC, 1 h; (v) $KHSO_5$. 0.5 $KHSO_4$. 0.5 K_2SO_4, $(CH_3)_2C{=}O/H_2O$ 25 ^oC, 2 h; (vi) Mg, I_2, THF, reflux, 1 h, (vii) $CH_3CH_2CHBrCO_2CH_3$, THF, reflux, 2 h; (viii) 3M KOH/CH_3OH, reflux, 2h, (ix)

CDI, $CH_3SO_2NH_2$, DBU, DCM, 25 ^oC, 4 h.

AKR1C3 and AKR1C2 Inhibitor Screening

Naproxen analogs were synthesized to explore the effect of modifications of its structure on AKR1C3 activity and selectivity. Based on the observation that other NSAIDs require the carboxylic acid group for optimal inhibition of the AKR1C enzymes,[44] most of the synthesized compounds retained this functional group. Modifications were made primarily on the chiral α-carbon or the 6–position of the naphthalene ring. Due to the presence of the chiral center in the molecule, most of compounds were initially assayed as racemates and screened for AKR1C2 and AKR1C3 inhibition without separation of the enantiomers.

The ability of the compounds to inhibit the $NADP^+$ dependent oxidation of *S*-tetralol catalyzed by AKR1C3 and AKR1C2 was determined and IC_{50} values obtained, **Figure 1** & **Table 1**. Since the *S*-tetralol assays were performed at K_m the IC_{50} values for the two enzymes were directly comparable. Naproxen inhibited AKR1C3 with an IC_{50} value of 180 nM and was not selective for AKR1C3 over AKR1C2, consistent with previous studies.[45] As naproxen, **1** is an *S*-enantiomer, its *R*-enantiomer, **1a** was evaluated for AKR1C3 inhibition and selectivity. *R*-naproxen inhibited AKR1C3 and AKR1C2 with IC_{50} values of 50 nM and 2.75 μM, respectively, which makes it more potent and more selective for AKR1C3 than naproxen**.** Replacement of the 6-*OMe* group of naproxen with an -*Et* to give **5,** or an -*OEt* to give **6,** did not change the potency and selectivity for AKR1C3. On the other hand, an isosteric replacement of the 6-*OMe* with the thiomethyl group, -*SMe* to give compound **9**, led to a 3-fold increase in the inhibitory potency for

AKR1C3 (IC_{50} = 60 nM) over that seen with naproxen while the AKR1C2 inhibitory potency remained unchanged. This translated to 25 fold selectivity for AKR1C3 over AKR1C2 by compound **9**. Because the -*SMe* group can be metabolized to the S(=O)Me and $S(=O)_2Me$ groups, compounds **10** and **11** containing these functional groups at the 6-position were synthesized and screened for AKR1C3 activity and selectivity**.** Compared to **9**, both compounds **10** and **11** displayed a greater than 15 fold loss of inhibitory potency on AKR1C3.

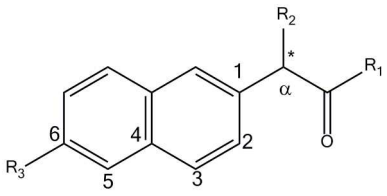

Figure 1. Structure of Naproxen Analogs

Table 1: Structure and AKR1C3/AKR1C2 Inhibitory Potency of Naproxen Analogs

Compound	R_1	R_2	R_3	AKR1C3 IC_{50} (μM) + S.E. (n= 4)	AKR1C2 IC_{50} (μM) + S.E. (n =4)	Ratio IC_{50} value (AKR1C2: AKR1C3)
S-Naproxen (**1**)	-OH	-Me	-OMe	0.18 ± 0.04	1.26 ± 0.15	7
R-Naproxen **(1a)**	-OH	-Me	-OMe	0.05 ± 0.004	2.75 ± 0.35	56
(±) 5	-OH	-Me	-Et	0.12 ± 0.0075	1.9 ± 0.11	15
(±) **6**	-OH	-Me	-OEt	0.10 ± 0.0076	2.4 ± 0.24	24
(±) **9**	-OH	-Me	-SMe	0.060 ± 0.0054	1.5 ± 0.14	25
(*R*) 9a	-OH	-Me	-SMe	0.05 + 0.0015	4.35 + 0.61	87
(*S*) 9b	-OH	-Me	-SMe	0.07 ± 0.004	1.35 ± 0.09	19
(±) **10**	-OH	-Me	-S(=O)Me	1.05 ± 0.13	6.3 ± 0.35	6
(±) **11**	-OH	-Me	$-S(=O)_2Me$	0.82 ± 0.1	3.0 ± 0.14	4
(±) **14**	-OH	-Et	-OMe	0.12 ± 0.014	7.6 ± 0.95	58
(*R*) **14a**	-OH	-Et	-OMe	0.11 ± 0.01	48.1 ± 5.0	437
(S) **14b**	-OH	-Et	-OMe	0.12 ± 0.01	1.72 ± 0.37	14
(±) **15**	$-NHSO_2Me$	-Et	-OMe	6.0 ± 1.0	34 ± 1.8	6
16[1]	-OH	-H	-OMe	0.65 ± 0.11	19.04 ± 3.7	29

[1]Windsor et al., ACS Med Chem Lett. 2012, 13 759-63

The *N*-(methylsulfonyl)acetamide analogue, **15** displayed a significant loss of inhibitory activity for AKR1C3 and AKR1C2 with IC_{50} values of 6.0 μM and 34 μM, respectively underscoring the need for a free carboxylic acid group for optimal inhibition of the AKR1C enzymes. Next, the replacement of the *α-Me* group of naproxen with an -*Et* gave **14,** which was the most AKR1C3 selective racemate evaluated. With an IC_{50} value of 120 nM against AKR1C3, compound **14** was more potent as an AKR1C3 inhibitor than naproxen and was 58 fold selective for AKR1C3 over AKR1C2. Due to its favorable properties the racemic mixture of **14** was separated to give the *R*- (**14a**) and the *S*- (**14b**) enantiomers. The configuration of the enantiomers was inferred by comparing the elution order of the enantiomers with that of naproxen and *R*-naproxen when the same chiral column and mobile phase was used (see supporting information). Surprisingly, while the AKR1C3 inhibitory potency of the enantiomers was similar and not significantly different from the inhibitory potency of the racemate, the AKR1C2 inhibitory potency of the enantiomers was markedly different. The *S*-enantiomer inhibited AKR1C2 with an IC_{50} of 1.72 μM while the *R*-enantiomer displayed an IC_{50} value of 46.4 μM against AKR1C2. This translated to 14- and 437-fold selectivity for AKR1C3 inhibition over AKR1C2, respectively. Eliminating the chiral center of naproxen by the removal of the *α-Me* group to give **16,** led to a loss of inhibitory potency and selectivity for AKR1C3 indicating the importance in retaining the *R*-configuration. The *R*- and *S*- enantiomers of compound **9** were also examined based on the selectivity achieved with the *R*-enantiomer **14a**. Compound **9a** showed 87-fold

selectivity for AKR1C3 which was 5-fold less than the selectivity observed with compound **14a**, demonstrating that the –OMe was preferred over the more bulky –SMe.

Compound **14a** was the most selective AKR1C3 inhibitor identified from the primary screen. When tested for inhibition of AKR1C1, it displayed selectivity for AKR1C3 over AKR1C1 inhibiting the latter with an IC_{50} value of 50 μM, which translates to a 500 fold selectivity for AKR1C3 (**Figure 2.**) Similar, selectivity was observed when the compound was screened against AKR1C4.

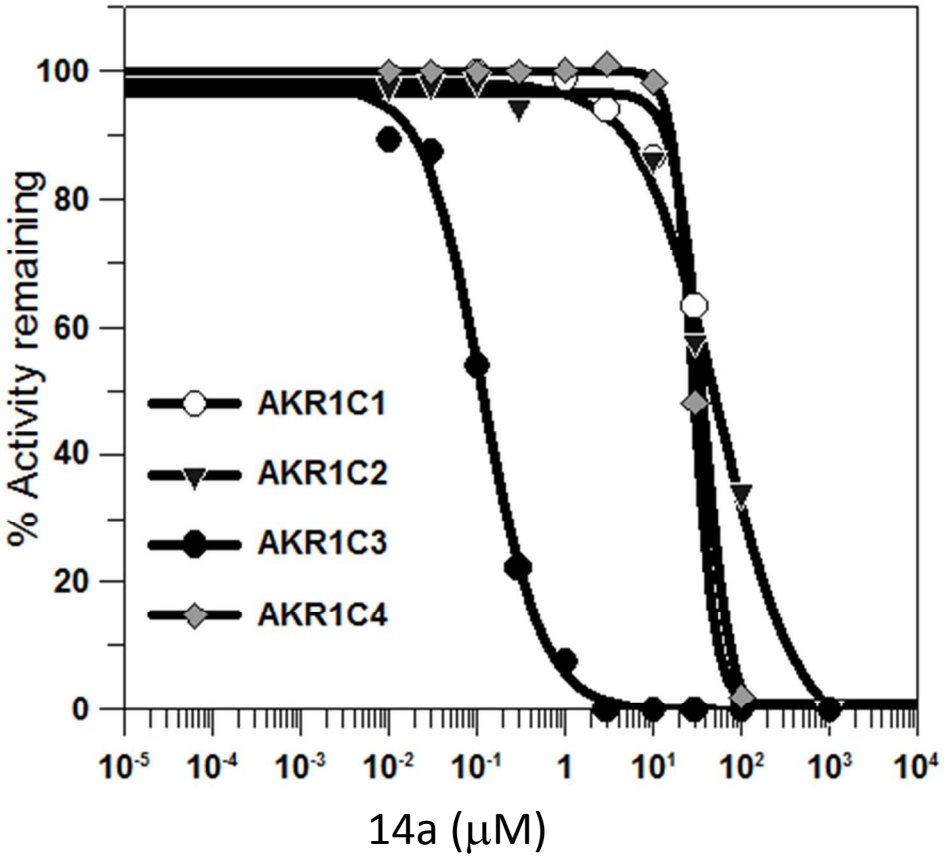

Figure 2. Inhibitory effect of compound **14a** on AKR1C1-4

Effect of 14a on AKR1C2 Catalyzed Reduction of 5α-DHT

Compounds **14a** and **14b** were next evaluated for the ability to inhibit AKR1C2 catalyzed NADPH dependent reduction of 5α-DHT. This was necessary to establish the lack of inhibitory activity on AKR1C2 using its physiologically relevant ketosteroid substrate. In this reaction, compound **14b** inhibited AKR1C2 in a dose dependent manner over the concentration range of 3 – 100 μM achieving 70% inhibition of enzyme activity at 100 μM (**Figure 3**). In contrast, **14a** did not display any significant inhibition of AKR1C2 at <100 μM concentrations. Flufenamic acid (FLU), a non-selective inhibitor of the AKR1C enzymes displayed about 70% inhibition of AKR1C2 at 10 μM concentration.

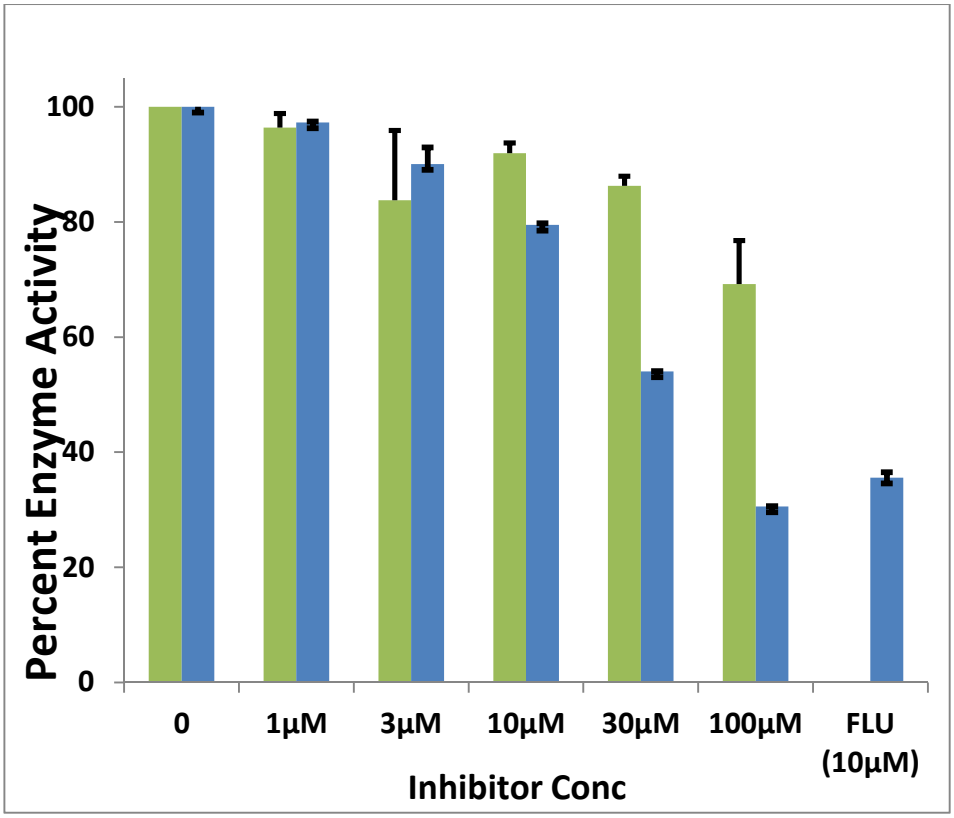

Figure 3: Effect of compounds **14a (green)** and **14b (blue) on** AKR1C2 catalyzed reduction of 5α-DHT.

Mode of AKR1C3 Inhibition by 14a

The pattern of AKR1C3 inhibition by **14a** was evaluated in by measuring the $NADP^+$ dependent oxidation of *S*-tetralol and by measuring the NADPH dependent reduction of Δ^4-androsten-3,17-dione. Compound **14a** competitively inhibited the AKR1C3 catalyzed oxidation of *S*-tetralol with a K_i value of 31 nM (**Figure 4a**). The same mode of inhibition was also observed when the reduction of Δ^4–AD was monitored, albeit with a much higher K_i value of 750 nM (**Figure 4b**).

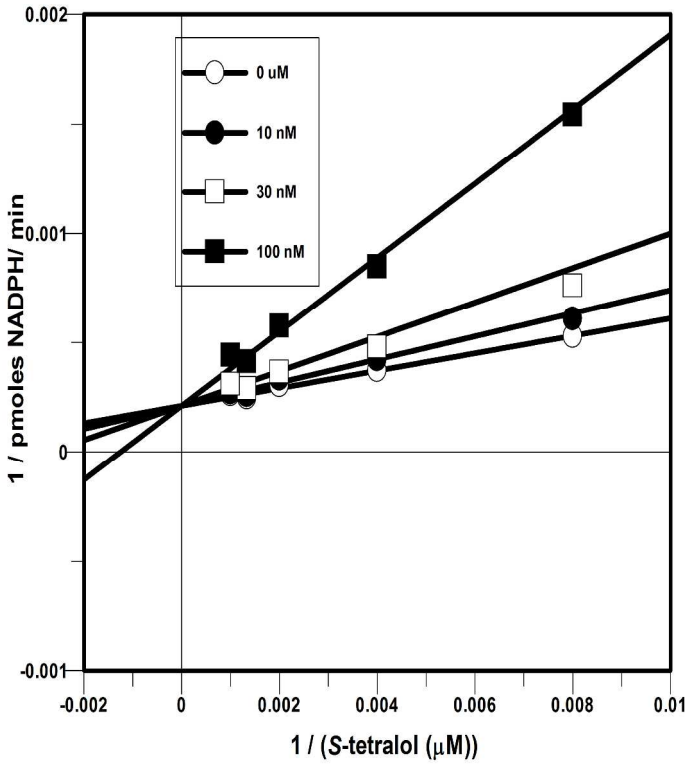

Figure 4a. Competitive Inhibition of AKR1C3 catalyzed oxidation of *S*-tetralol by **14a**

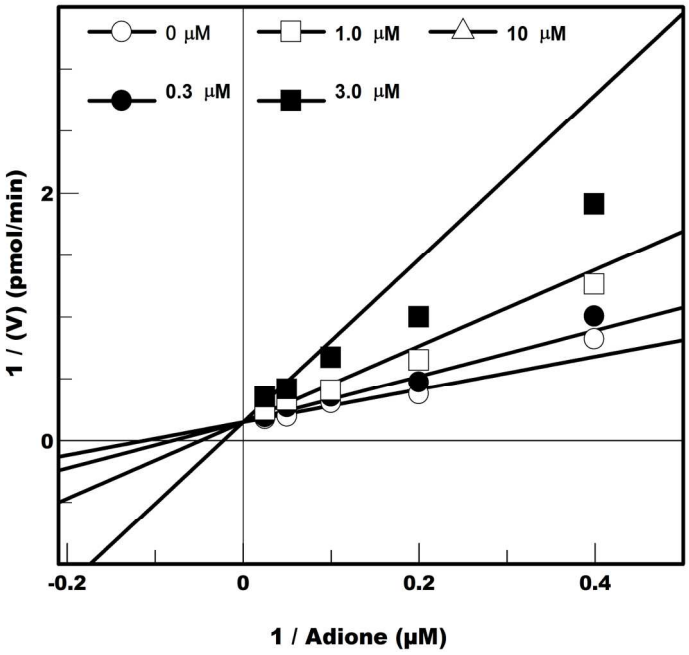

Figure 4b. Competitive Inhibition of AKR1C3 catalyzed Reduction of Δ^4–AD by **14a**

Inhibition of COX-1

Naproxen inhibited COX-1 with an IC_{50} value of 61 nM. Relative to naproxen, **14b** displayed a 30 fold loss of inhibitory potency on COX-1 with an IC_{50} value of 1.93 μM (**Figure 5**). There was a profound loss of inhibitory activity on COX-1 activity by the respective *R*-enantiomers, compounds **1a** and **14a.** Both compounds displayed less than 20% inhibition of COX-1 activity at the highest inhibitor concentration (100 μM) tested. This is consistent with reported structure activity relationship studies on the COX-1 inhibitory effects of naproxen and its analogs.

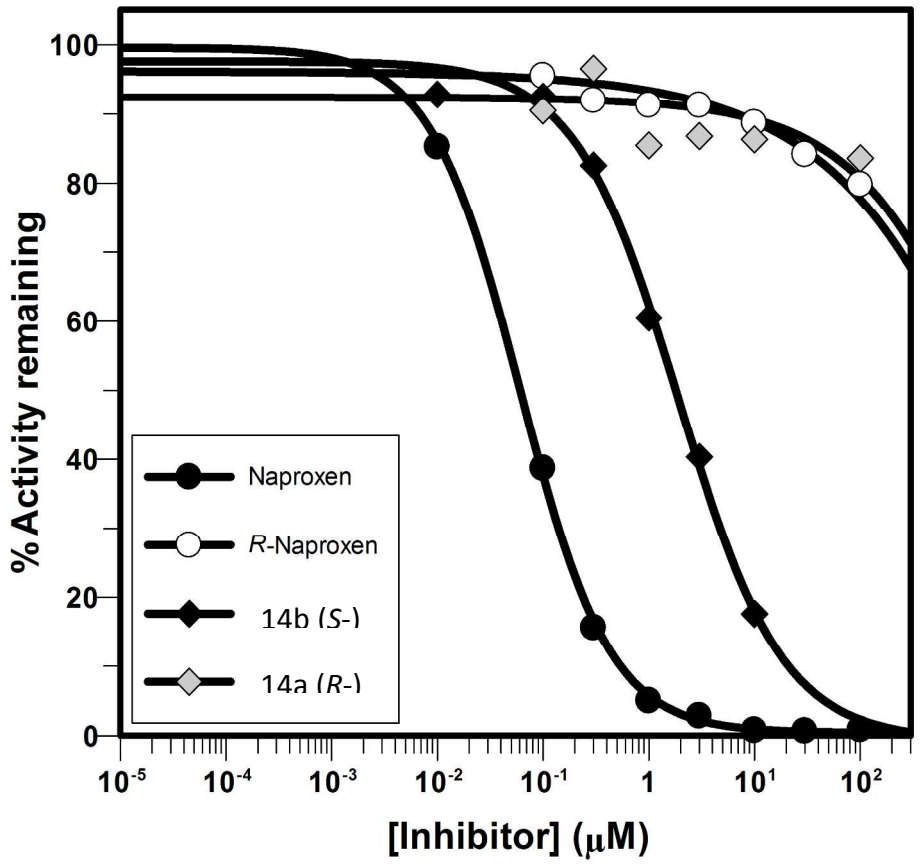

Figure 5. Inhibition of COX-1 by naproxen analogs

Table 2. Inhibitory potency of compounds on AKR1C3 and COX-1

Compound	**AKR1C3 IC_{50} (μM)**	**COX-1 IC_{50} (μM)**	**COX-2 IC_{50} (μM)**	**Ratio (COX-1 IC_{50} : AKR1C3 IC_{50})***	**Ratio (COX-2 IC_{50} : AKR1C3 IC_{50})**
Naproxen 1	0.18	0.061	0.90	0.34	15
R-naproxen 1a	0.05	>100	>25	>2000	>500
14a	0.11	>100	No inhibition*	>910	∞
14b	0.12	1.93	No inhibition*	16	∞

*Taken from Duggan et al. J. Biol. Chem. 285 (2010) 34950 (ref. 42).

A comparison of inhibitory potency of the compounds against AKR1C3 and COX-1 (**Table 2**) shows that **14a** was almost a thousand fold more selective for AKR1C3 over COX-1. Compound **14** which is a racemate of **14a** and **14b** had no inhibitory activity on COX-2 at the maximum concentration of arachidonic acid tested as substrate (10 μM).

Effect on AR Reporter Gene Assay:

Compound **14a** was next evaluated for a direct effect on AR signaling. Compound **14a** did not effect the *trans*-activation of the AR mediated by 5α-DHT There was a concentration-dependent increase in luciferase activity when HeLa13 cells containing a stably transfected AR and an androgen response element driven luciferase gene were treated with increasing concentrations of 5α-DHT. The luciferase activity peaked at 0.3 nM 5α-DHT, however, there were no significant change in the 5α-DHT induced luciferase expression when cells were treated with increasing concentrations of 5α-DHT in the presence of 10 μM compound **14a**, **Figure 6.**

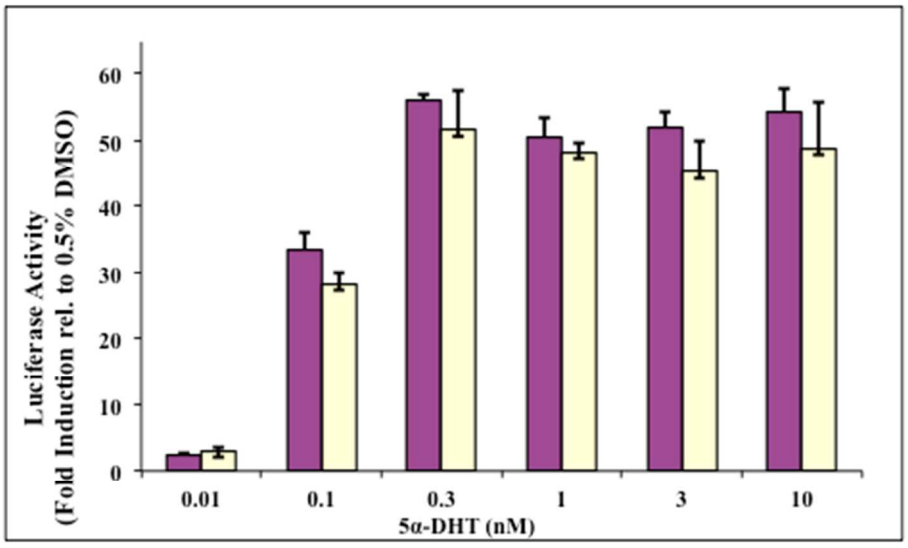

Figure 6: Effect of Compound **14a** on DHT Induced AR Gene Expression. DHT alone (purple) and DHT plus 10 μM compound **14a**

Inhibition of AKR1C3-mediated Production of Testosterone

LNCaP-AKR1C3 cells were used to probe the metabolism of Δ^4–AD in the presence and absence of compound **14a**. Radio-labeled [^{3}H]-Δ^4-AD was incubated with carrier Δ^4–AD (100 nM) with LNCaP-AKR1C3 cells placed in medium supplemented with charcoal dextran stripped fetal bovine serum (CD-FBS) which is devoid of androgens. Androgens were extracted after 48 hrs and the aqueous fraction subject to β-glucuronidase treatment to liberate androgen conjugates that we have previously shown to exist due to the robust uridine-5'-diphospho-glucuronosyltransferse (UGT) activity in these cells. Metabolites were separated by radiochromatography using TLC. LNCaP-AKR1C3 cells were able to metabolize [^{3}H]-Δ^4-AD to [^{3}H]-androsterone glucuronide and [^{3}H]-testosterone glucuronide. However, in cells that were treated with 30 μM of compound **14a,** the production of [^{3}H]-testosterone glucuronide was significantly inhibited (**Figure 7**).

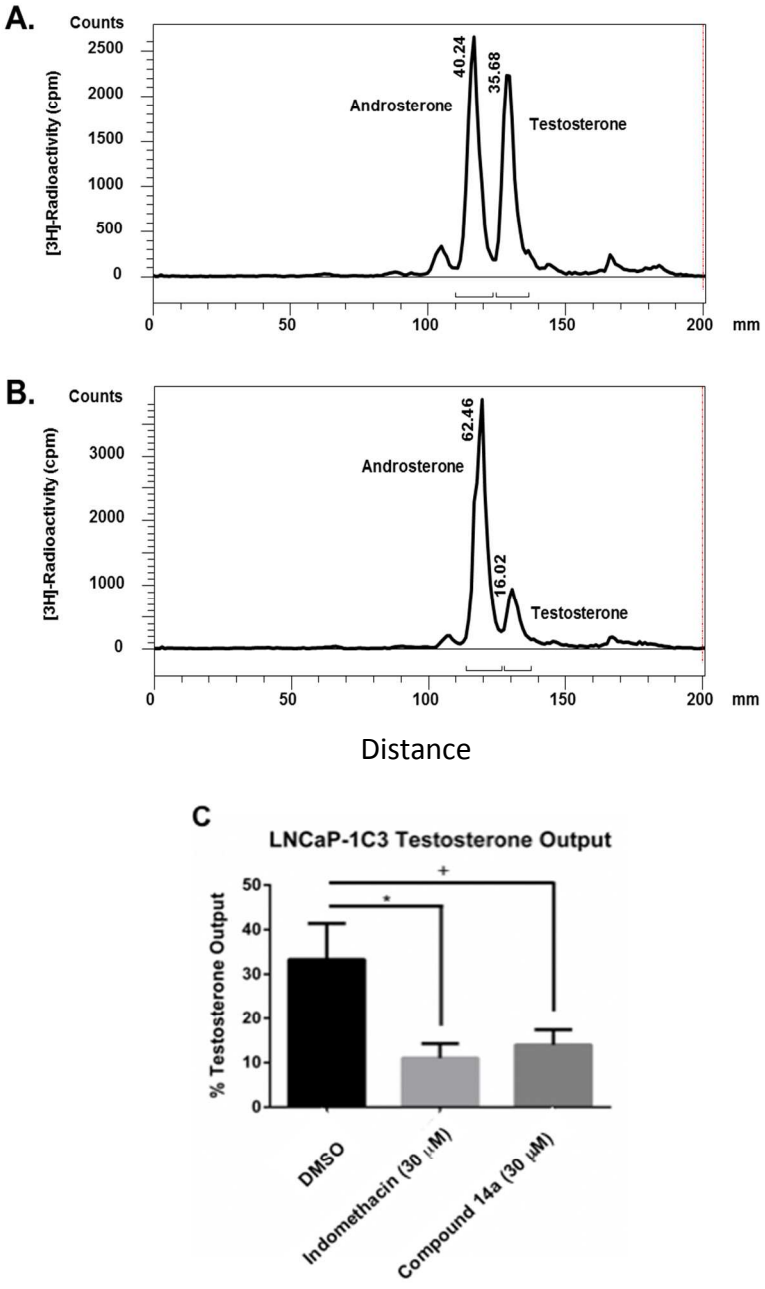

Figure 7: Inhibition of testosterone formation in LNCaP-1C3 cells with Compound **14a**. Panel A shows conversion of 100 nM Δ^4-AD to testosterone in LNCaP-AKR1C3 cells following digestion with β-glucurondiase. Panel B, shows the same experiment performed in the presence of 30 μM compound **14a;** Panel C shows statistical analysis of n=3 versus indomethacin as a positive control * p value < 0.001; p value = 0.001

Inhibition of AKR1C3 Mediated AR Gene Expression:

Compound **14a** was also tested for its ability to block the Δ^4-AD mediated expression of PSA in LNCaP-AKR1C3 cells by western blot analysis **Figure 8**. Treatment of these cells with 100 nM Δ^4–AD led to a robust increase in PSA expression. This increase in PSA was reduced when the cells were treated with 100 nM Δ^4–AD in the presence of 30 μM of compound **14a**.

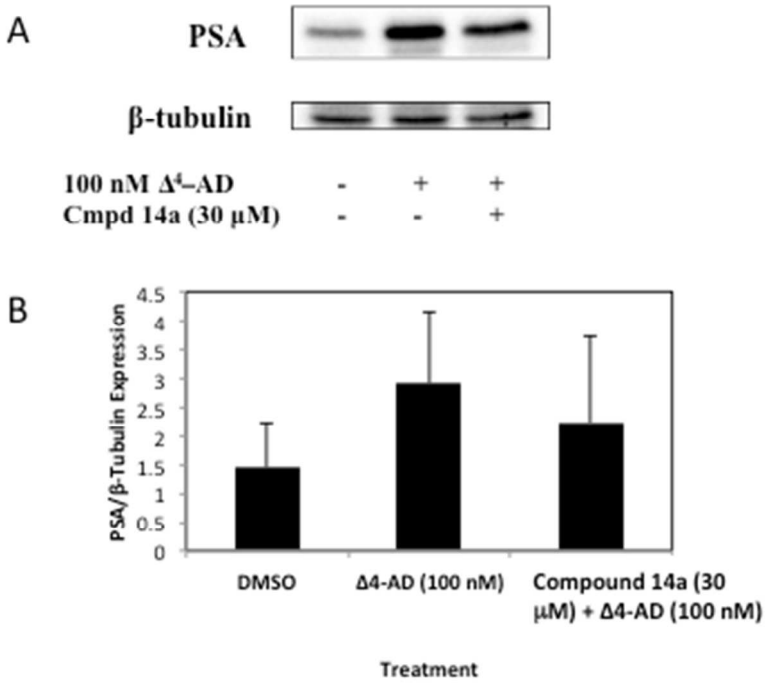

Figure 8: Inhibition of Δ^4–AD induced PSA expression in LNCaP-AKR1C3 cells by compound 14a. Panel A, immunoblot; Panel B, densitometric traces of immunoblots with normalization of PSA to β-tubulin for biological replicates (n=3).

DISCUSSION

CRPC is currently treated with either AA or ENZ, however, patients rapidly develop drug resistance leading to an increase in median survival time of only 3- 4 months. One mechanism of drug resistance is overexpression of AKR1C3. AKR1C3 represents a rational target due to its vital role as "gatekeeper" for the production of potent androgens regardless of the pathway used and its ability to function as a coactivator for the AR. This underscores the intense attention the search for AKR1C3 inhibitors has generated. [30, 36,37, 46-53]

NSAIDs are known to be pan inhibitors of the AKR1C enzymes. This is thought to be as a result of the interaction of the carboxylate groups of NSAIDs with the catalytic site of the AKR1C enzymes.[53] The inhibition of AKR1C3 by NSAIDs is attained at therapeutic concentrations that are required for COX inhibition. This makes using these compounds as leads a promising approach since the resulting analogs may have similar pharmacokinetic profiles and therefore may be well tolerated. We have conducted structure activity relationship studies on the NSAID, naproxen and identified a *R*-enantiomer that differs from *R*-naproxen by the simple substitution of an ethyl group for a methyl group with therapeutic potential for CRPC.

The presence of small lipophilic groups at the 6-position of naproxen is optimal for COX inhibitory activity. [54] To determine the contribution of the 6-*OMe* group to the inhibitory potency of naproxen for AKR1C3, analogs with small substituents were synthesized and evaluated. With the exception of the 6-*SMe*, all the other substituents at the 6-position did not significantly improve AKR1C3 potency or selectivity.

All the compounds evaluated were superior inhibitors of AKR1C3 than AKR1C2. Since the AKR1C enzymes differ primarily in the enzyme subpockets, it is likely that the larger and more flexible subpockets of AKR1C3 allow for better interaction with the enzyme.[44.56]

Naproxen, with a chiral center at the α-carbon is used as the *S*-enantiomer for anti-inflammatory activity. This is due to the *R*-enantiomer being significantly less active as a COX inhibitor, **Figure 5**. [42,54] Naproxen is likewise a potent AKR1C3 inhibitor. However, *R*-naproxen, compound **1a** has never been evaluated for AKR1C3 inhibitory activity. Relative to naproxen, compound **1a** was found to be more potent as an AKR1C3 inhibitor and less potent as an AKR1C2 inhibitor which translated into an increased selectivity for AKR1C3 relative to AKR1C2. The higher affinity of **1a** over naproxen for AKR1C3 is supported by crystallographic studies conducted by Flanagan et al. [48] These authors reported that while both *S*- and *R*-naproxen bind to AKR1C3 when the respective enantiomers were soaked separately into preformed crystals of the AKR1C3.$NADP^+$ complex, only the *R*- enantiomer was bound in the these crystals when co-soaked with both enantiomers. This observation was attributed to the number of intermolecular interactions made by the enantiomers with the enzyme despite having relatively similar binding poses with AKR1C3. Relative to naproxen, *R*-naproxen made more contacts with side chains in the active site and cofactor leading to a greater complementarity.[48] This would suggest the existence of stereochemical specificity in the interaction of *R*-profens with AKR1C3 and loss of specificity with AKR1C2. To further explore this observation, compound **14** with an α-*Et* group and its respective enantiomers **14a**(*R*-) and **14b**(*S*-)

were subsequently evaluated. Surprisingly, the expected stereochemical specificity was not apparent in the interaction of the enantiomers, **14a** and **14b** with AKR1C3 but was observed with AKR1C2 as the two enantiomers displayed markedly different inhibitory potency towards AKR1C2. The different inhibitory potency of the enantiomers on AKR1C2 was subsequently confirmed using a steroidal substrate for AKR1C2. Modeling studies of enantiomers, **14a** and **14b** indicate that they adopt remarkably distinct binding poses with AKR1C2, (see **Figure 9 & 10**).

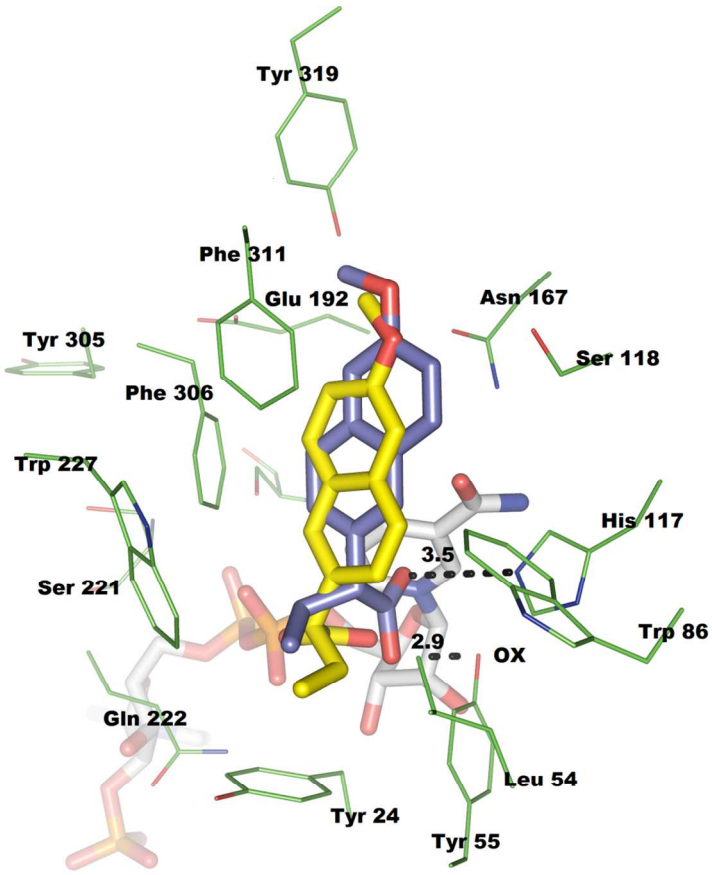

Figure 9. Alignment of 14b and 14a in the AKR1C3 active site. AKR1C3 residues (green); **14b** (yellow), **14a** (purple), Dotted line: possible hydrogen bond; OX: oxyanion site (residues highlighted in pink), Ligand alignments were performed using LigAlign plugin in Pymol. The template crystal structures of the AKR1C3•$NADP^+$ complexes were chosen from the RCSB protein data bank (PDB code: 3UFY and 3R58) [also see Supporting Information].

Ligand alignments of enantiomers **14a** and **14b** to the existing crystal structures (3UFY and 3R58) indicate that they adopt similar binding poses with AKR1C3 (Figure 9). Both Analogs **14a** and **14b** show a similar binding mode to that of *R*-naproxen with the ethyl group occupying the sub pocket 3 (SP3) formed by residues Tyr-24, Glu-192, Ser-217, Ser-221, and Gln-222. [47] The remainder of the molecule extends into the Sub pocket 1 (SP1) pocket composed of Ser-118, Asn-167, Phe-306, Phe-311, and Tyr-319. The ligand alignments revealed closer proximity of carboxylic group of **14a** compared to **14b** at the oxyanion site (Tyr-55, His-117, and the NADP+ cofactor). A slight increase in inhibitory potency and selectivity of **14a** may be due to the favorable H-bond interaction with the oxyanion site.

Compounds **14a** and **14b** display remarkably different binding poses to each other with AKR1C2 (**Figure 10**). While analog **14a** binds in the active site of AKR1C2 similar to AKR1C3, compound **14b** further extends into the SP3 pocket with no interaction with the SP1 pocket. When the structures of AKR1C2 and AKR1C3 with either **14a** or **14b** bound were overlaid additional reasons for the AKR1C3 selectivity of compound **14a** were found. The Leu 308 side chain at the AKR1C2 binding site sterically clashes with **14a,** which may significantly decrease its preference towards binding in the SP1 pocket of AKR1C2, resulting in a loss of inhibitory potency for AKR1C2.

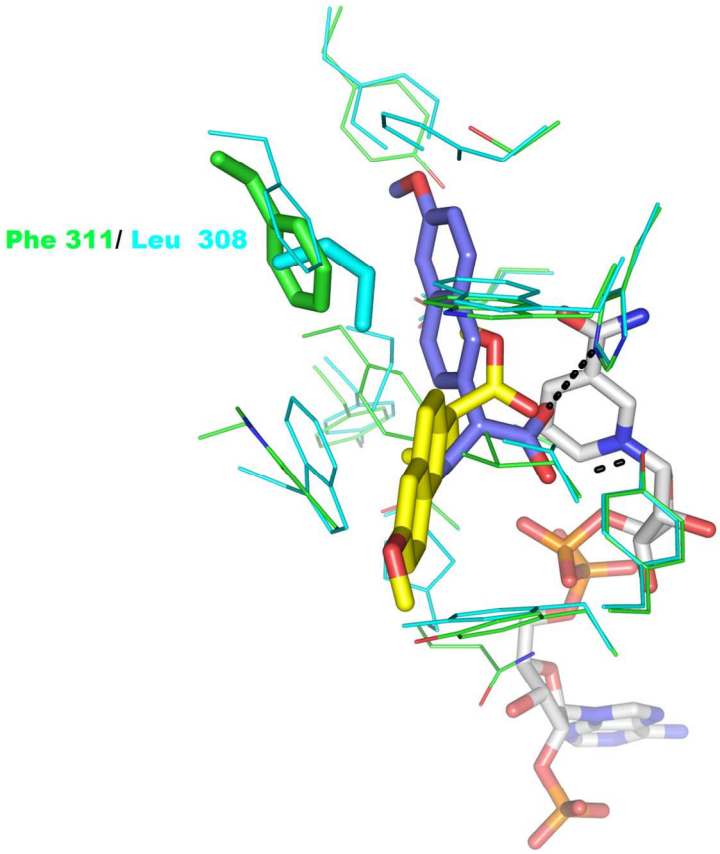

Figure 10. Comparison of 14b and 14a binding to AKR1C2 and AKR1C3 The **14b** (yellow) and **14a** (purple) binding modes in AKR1C2 (cyan) and AKR1C3 (green). The template crystal structure of the AKR1C2.NADP+ complex was taken from the RCSB protein data bank (PDB code: 4JQ1) [also see Supporting Information].

Compound **14a** competes with *S*-tetralol and the physiologically relevant steroidal substrate, Δ^4–AD for binding to AKR1C3, albeit with different binding constants. The difference in binding constant is related to the formation of two different inhibitor complexes. [34] During the competitive inhibition of *S*-tetralol oxidation the E.NADP$^+$.I complex forms (where I = inhibitor) to yield a K_i = 31 nM for **14a**. By contrast during the competitive inhibition of Δ^4–AD reduction the E.NADPH.I complex forms to yield a K_i

= 750 nM for **14a**. Thus compound **14a** displays a 20-fold preference for the E.NADP$^+$ complex, **Figure 11.** Which complex is inhibited in cells is unclear.

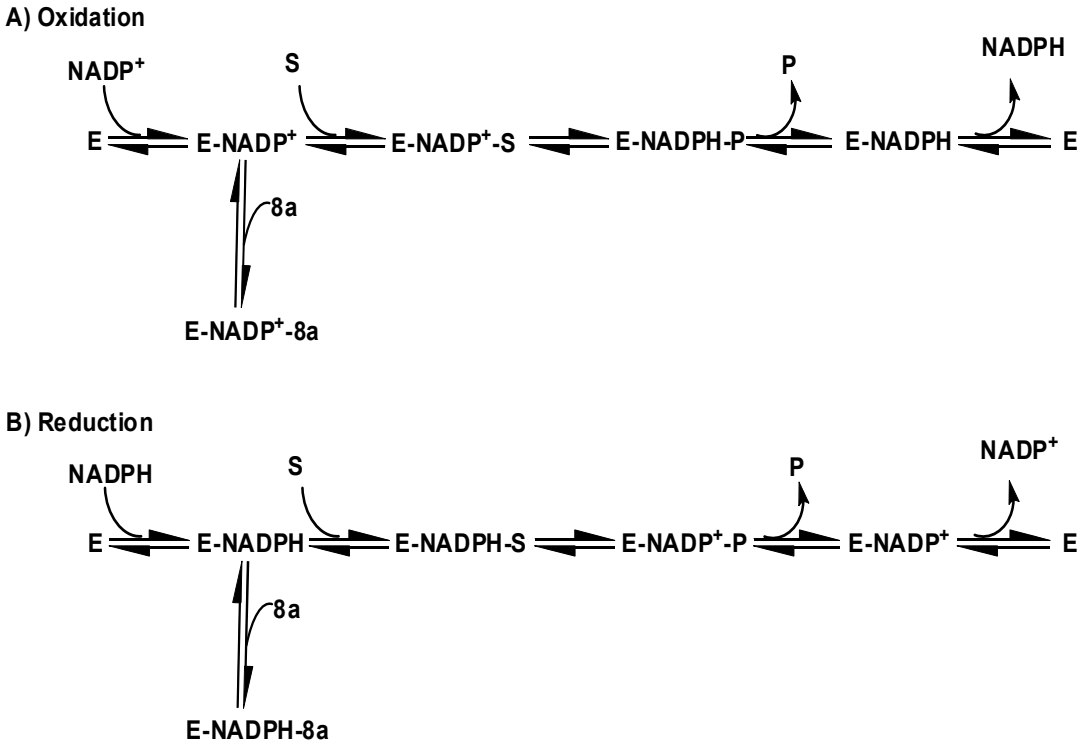

Figure 11. Kinetic mechanism of the reactions catalyzed by AKR1C3. (A) oxidation reaction where the substrate S is *S*-tetralol and the product P is tetralone; and (B) reduction reaction where the substrate is Δ^4-androstene-3,17-dione and the product is testosterone. S= substrate, P = product and E= enzyme.

Indomethacin, another NSAID has been shown to have greater affinity for the E.NADP$^+$ complex presumably due to the interaction between the negative charge on the compound and the positive charge of NADP$^+$.[44] Since most AKR1C3 inhibitors that have

a carboxylic acid group are anchored to the enzyme's catalytic site via this functional group, [37, 47, 48, 56, 57] compound **14a** with a negatively charged carboxylic acid group at pH 7 will likewise be expected to have similar interaction. This would bring the negative charge of **14a** close to the cofactor where it will form a stronger interaction with $NADP^+$ relative to NADPH. The stronger interaction between **14a** and $NADP^+$ would account for the lower K_i value obtained for **14a** during the oxidation of *S*-tetralol by AKR1C3 when compared to the value obtained during the reduction of Δ^4–AD by AKR1C3.

Compound **14a,** had no effect on the transactivation of the AR mediated by 5α-DHT in HeLa cells. These cells were also shown to express AKR1C3 endogenously (Adeniji and Penning, unpublished). Thus if AKR1C3 acts as an AR coactivator in these cells then compound **14a** differs from GTx560 in that it does not block co-activator function[30]. This would suggest that not all competitive inhibitors of AKR1C3 are able to inhibit the co-activator function of this protein. However, co-activator function and its inhibition can be cell context dependent.

Consistent with the stereoselective inhibition of COX observed with naproxen, compound **14a** was likewise devoid of inhibitory activity on COX which is essential since chronic COX inhibition is not desirable in the context of CRPC management. We anticipate that due to the close structural similarity of naproxen with compound **14a** where the methyl group of *R*-naproxen was simply replaced by an ethyl group in compound **14a**, that compound **14b** would have favorable absorption, distribution, metabolism, elimination and toxicological (ADMET) properties that would enable its

rapid transit into man. However, it is recognized that the addition of the extra methylene group may effect the compounds lipohilicity and hence affect these properties.

We also note with interest that (*R*)-profens are substrate-selective inhibitors of endocannabinoid oxygenation by COX-2 and suggest that they will have analgesic benefit by this mechanism.[42,43] As a consequence (*R*)-profens in CRPC may not only inhibit intratumoral androgen synthesis but may alleviate pain associated with the metastatic disease.

Conclusion

We have identified (*R*)-2-(6-methoxynaphthalen-2-yl)butanoic acid as a potent AKR1C3 inhibitor. This compound competitively inhibits AKR1C3 and displays selectivity for AKR1C3 over other AKR1C enzymes and COX. It was also efficacious at blocking AKR1C3 in a LNCaP-AKR1C3 cells which is a model for CRPC cells. This compound represents a potential therapeutic agent that can be used in the management of CRPC either alone or in combination with AA or ENZ where it may improve efficacy and reduce the incidence of resistance to these drugs.

EXPERIMENTAL SECTION

Chemistry

General-All commercially available reagents and anhydrous solvents were ACS grade or better and were used as received.

Analytical thin-layer chromatography was carried out using glassbacked plates coated

with fluorescent silica gel 60 F254 from Whatman (Partisil LK6D). Spots were visualized under natural light and UV illumination at λ = 254 and 365 nm. Flash chromatography was conducted on a Biotage SP1 automated flash chromatography system equipped with a fixed wavelength UV detector (λ = 254 nm). Samples were preabsorbed onto ready-made silica gel samplets and then applied on to normal-phase flash chromatography cartridges (Biotage KP-SIL, size according to requirements) and elution with a 0−100% EtOAc/hexane (0.5% acetic acid) gradient. ^{1}H and ^{13}C NMR spectra were recorded at 400 and 100 MHz, respectively, using a Bruker AV-400

with sample changer (BACS 60). A purity of ≥95% (unless otherwise indicated) for the final compounds in this study was confirmed by analytical HPLC on a Waters HPLC system with PDA detector (set at λ = 254 nm) equipped with a Supelco Supelcosil LC-18 reverse-phase column (15 cm Å~ 3 mm, 5 μm). Compounds screened in the current study also were characterized with respect to their m.pt. and HRMS.

Preparation of Compounds

***(S)*-Methyl 2-(6-(trifluoromethylsulfonyloxy)naphthalen-2-yl)propanoate, 4.** To (*S*)-naproxen (**1**, 3 g, 13 mmol) in acetic acid (20 mL) was added 48% HBr (11.2 g, 7.5 mL, 138 mmol) at 0 ^{o}C. [57] Following 3 h of reflux, water (40 mL) was added to precipitate out the product **2** which was isolated by filtration. To the crude product **2** was added methanol (35 mL) and TMSCl (1.7 g, 2.0 mL, 15.7 mmol), and the mixture was stirred at room temperature for 2 hours.[58, 59] The solvent was removed *in vacuo* resulting in a tan solid **3,** which was dissolved in CH_2Cl_2 (20 mL). Following the addition of triethylamine

(2.6 g, 3.6 mL, 26.1 mmol) at 0 ^{o}C, trifluoromethanesulfonic anhydride (2.8 g, 2.7 mL, 15.7 mmol) was added dropwise, and the mixture was warmed to room temperature and allowed to stir for 1 hour. The mixture was then diluted with diethyl ether, quenched with 1 M HCl, and washed with saturated sodium bicarbonate and brine. The organic layer was dried over $MgSO_4$ and then concentrated, resulting in the desired product **4** (4.5 g, 95 %). ^{1}H NMR (400 MHz, $CDCl_3$) δ 1.57 (d, 3H), 3.65 (s, 3H), 3.89 (q, 1H), 7.34 (dd, *J* = 4, 8 Hz, 1H), 7.52 (dd, *J* = 4, 8 Hz, 1H), 7.70 (d, *J* = 4 Hz, 1H), 7.77 (s, 1H), 7.81 (d, *J* = 8 Hz, 1H), 7.86 (d, *J* = 8 Hz, 1H); MS *m/z*: 363 $(M + H)^{+}$.

2-(6-Ethylnaphthalen-2-yl)propanoic acid, 5. (*S*)-Methyl 2-(6-(trifluoromethylsulfonyloxy)naphthalen-2-yl)propyl ester **3** (4.2 g, 11.6 mmol) and 1 M of cesium carbonate (20 mL) were added to a solution of potassium vinyltrifluoroborate (2.4 g, 17.5 mmol) in EtOH (100 mL). Then tetrakis(triphenylphosphine) palladium (672 mg, 0.59 mmol) and triethylamine (2.4 g, 3.2 mL, 23.8 mmol) were added to the mixture and stirred 50 ^{o}C for 16 hours. The reaction mixture was cooled to room temperature, water (100 mL) was added and the resulting mixture was stirred at room temperature for 30 minutes. The reaction mixture was filtered resulting in (*S*)-methyl 2-(6-vinylnaphthalen-2-yl)propanoate as a brown solid (2 g), which was used directly to the next step without further purification. To a round bottom flask purged with argon was added THF (35 mL), palladium(II) acetate (52 mg, 0.24 mmol), and tri-*tert*-butyl phosphine (94 mg, 113 mL, 0.46 mmol). This was brought to reflux and allowed to stir for 30 minutes. The reaction was then cooled and (*S*)-methyl 2-(6-vinyl naphthalen-2-yl)propanoate (2 g, 8.9 mmol) and formic acid (2.7 g, 2.3 mL, 59 mmol) were added to

the reaction mixture. The mixture was again brought to reflux for 30 minutes, then cooled to room temperature, and allowed to stir for 12 hours. The reaction mixture was filtered through a bed of Celite and then concentrated *in vacuo* to give the crude (*S*)-methyl 2-(6-ethylnaphthalen-2-yl)propanoate (700 mg) which was added to 14 mL of a 3M KOH solution in MeOH. The reaction was held at reflux for 3 hours, then cooled and quenched with water. The reaction mixture was extracted with ethyl ether (3x). The aqueous layer was then acidified with 1 M HCl and then extracted into ethyl ether (3x), washed with brine, dried with $MgSO_4$, and concentrated under reduced pressure to give a crude residue, which was purified by column chromatography (n-Hex:EtOAc 4:1) to afford the pure racemic product **5** (450 mg, yield 94% last step, purity 99.4%, HPLC retention time 11.93 min, melting point 120-122 ^{o}C). ^{1}H NMR (600 MHz, DMSO-d_6) 1.18 (t, J = 5.5 Hz, 3H), 1.38 (d, J = 6 Hz, 3H), 2.68 (q, J = 4.5 Hz, 2H), 3.75 (q, J = 4.5 Hz, 1H), 7.30 (dd, J = 7.5, 2.5 Hz, 1H), 7.34 (dd, J = 7.5, 2.5 Hz, 1H), 7.58 (s, 1H), 7.66 (s, 1H), 7.71-7.73 (m, 2H); ^{13}C NMR (150.9 MHz, DMSO-d_6) 15.98, 18.90, 28.75, 45.19, 125.47, 125.94, 126.43, 127.74, 127.92, 128.03, 131.98, 132.70, 138.41, 141.66, 175.86; HRMS: *m/z* calcd for $C_{15}H_{16}O_2$ $(M-H)^-$ 227.1078; found 227.1079.

2-(6-Ethoxynaphthalen-2-yl)propanoic acid, 6. Potassium hydroxide (828 mg, 14.8 mmol) in 4 mL of methanol was added to a round bottom flask. (*S*)-methyl 2-(6-hydroxynaphthalen-2-yl)propyl methyl ester **3** (2.3 g, 9.8 mmol) in DMF (25 mL) was then added to the flask. The reaction was then allowed to stir at room temperature for 30 minutes. Iodoethane (3.0 g, 1.5 mL, 19.6 mmol) was added which was allowed to stir at room temperature for 3 hours. The reaction mixture was quenched with water and

extracted with CH_2Cl_2 (3x), the organic layer was then dried over $MgSO_4$, filtered, and finally concentrated *in vacuo* the crude product as a yellow solid (450 g), to which was added 8 mL of a 3M KOH solution in MeOH. The reaction was held at reflux for 2 hours, then cooled and quenched with water. The reaction mixture was extracted with ethyl ether (3x). The aqueous layer was then acidified with 1 M HCl and then extracted into ethyl ether (3x), washed with brine, dried with $MgSO4$, and concentrated under reduced pressure to give pure racemic product as an off-white solid **6** (360 mg, yield 85 % last step, purity 98%, HPLC retention time 11.28 min, melting point 148-150 ^oC). ^1H NMR (600 MHz, DMSO-d_6) 1.44 (t, J = 6 Hz, 3H), 1.49 (d, J = 6.5 Hz, 3H), 3.85 (q, J = 4.5 Hz, 1H), 4.19 (q, J = 4.5 Hz, 1H), 7.20 (dd, J = 2, 8.5 Hz, 1H), 7.32 (d, J = 2 Hz, 1H), 7.44 (dd, J = 2, 8.5 Hz, 1H), 7.76 (s, 1H), 7.78 (d, J = 8.5, 1H), 7.85 (d, J = 8.5, 1H); ^{13}C NMR (150.9 MHz, DMSO-d_6) 15.10, 18.92, 45.06, 63.54, 106.83, 119.37, 126.00, 126.83, 127.28, 128.80, 129.56, 133.73, 136.74, 156.79, 175.95; HRMS: *m/z* calcd for $C_{15}H_{16}O_3$ $(M-H)^-$ 243.1027; found 243.1026.

***(S)*-Methyl 2-(6-(triisopropylsilylthio)naphthalen-2-yl)propanoate, 7.** To a solution of (*S*)-methyl 2-(6-(trifluoromethylsulfonyloxy)naphthalen-2-yl)propyl methyl ester **4** (3 g, 8.3 mmol) in benzene (20 mL) was added $Pd(PPh_3)_4$ (0.95 g, 0.8 mmol) and sodium triisopropylsilanethiolate [60] (2.1 g, 9.9 mmol) dissolved in THF (10 mL). The solution was refluxed for four hours, then quenched with water and extracted with ethyl acetate. The organic layer was dried over $MgSO_4$ and concentrated. The crude product was purified by flash chromatography using 10:1 hexane:ethyl acetate to give pure product (2.9 g, 87 %). ^1H NMR (400 MHz, $CDCl_3$) δ 1.10 (d, 18 H), 1.25 (m, 3H), 3.65 (s, 3H),

3.86 (q, 1H), 7.31 (m, 2H), 7.41 (dd, J = 4, 8 Hz, 1H), 7.54 (dd, J = 4, 8 Hz, 1H), 7.67 (m, 2H); MS *m/z*: 403 $(M + H)^+$.

(*S*)-Methyl 2-(6-(methylthio)naphthalen-2-yl)propanoate, 8. To 15 mL of THF was added (*S*)-methyl 2-(6-(triisopropylsilylthio)naphthalen-2-yl)propanoate **7** (2.5 g, 6.2 mmol) followed by tetrabutylammonium fluoride (3.3 g, 3.6 mL, 12.4 mmol). The mixture was allowed to stir at room temperature for 2 hours. Methyl iodide (2.6 g, 1.2 mL, 18.6 mmol) was then added, and the resulting mixture was stirred for an additional 2 hours at room temperature. The reaction mixture was extracted with ethyl ether, dried over $MgSO_4$, and concentrated *in vacuo*. The crude product **8** was purified by flash chromatography using 7:1 hexane:ethyl acetate to give pure product (1.2 g, 75 %). ^{1}H NMR (400 MHz, $CDCl_3$) δ; 1.58 (d, 3H), 2.57 (s, 3H), 3.67 (s, 3H), 3.87 (q, 1H), 7.37 (dd, J = 4, 8 Hz, 1H), 7.42 (dd, J = 4, 8 Hz, 1H), 7.58 (s, 1H), 7.67 (s, 2H), 7.70 (d, J = 8Hz, 1H); MS *m/z*: 261 $(M + H)^+$

2-(6-(Methylthio)naphthalen-2-yl)propanoic acid, 9. To (*S*)-methyl 2-(6-(methylthio)naphthalen-2-yl)propanoate **8** (975 mg, 3.7 mmol) was added 20 mL of a 3 M KOH solution in MeOH. The reaction was refluxed for 2 hrs, cooled and then quenched with water. Following extraction with ethyl ether, the aqueous layer was acidified with 1 M HCl and then extracted into ethyl ether, washed with brine, dried with $MgSO_4$, and concentrated under reduced pressure to give pure product **9** (876 mg, yield 95 %, purity 99.1%, HPLC retention time 11.39 min, melting point 172-174 ^{o}C). ^{1}H NMR (600 MHz, DMSO-d_6) δ 1.45 (d, J = 6.5 Hz, 3H), 2.57 (s, 3H), 3.82 (q, J = 5 Hz, 1H), 7.38 (dd, J = 2, 8.5 Hz, 1H), 7.45 (dd, J = 2, 8.5 Hz, 1H), 7.68 (s, 1H), 7.74 (s, 1H),

7.79-7.82 (m, 2H); ^{13}C NMR (150.9 MHz, DMSO-d_6) 15.12, 18.85, 45.18, 63.54, 122.67, 125.84, 127.19, 127.32, 128.47, 131.14, 133.02, 136.13, 138.55, 175.79; HRMS: *m/z* calcd for $C_{14}H_{14}O_2S$ $(M-H)^-$ 245.0642; found 245.0637.

2-(6-(Methylsulfinyl)naphthalen-2-yl)propanoic acid, 10. 2-(6-(Methylthio)naphthalen-2-yl)propanoic acid **9** (65 mg, 0.26 mmol) was dissolved in 8 mL of dichloromethane. To this solution was added m-chloroperoxybenzoic acid (64mg, 0.29 mmol), which was allowed to stir at 0 ^{0}C for 1 hour. The reaction mixture was extracted with ethyl ether, dried over $MgSO_4$, and concentrated *in vacuo*. The crude product was purified by flash chromatography using 10:1 dichloromethane:methanol to give pure product **10** (46 mg, yield 62 %, purity 98.6%, HPLC retention time 7.16 min, melting point 130-132 ^{o}C). ^{1}H NMR (600 MHz, DMSO-d_6) δ; 1.40 (d, J = 6.5 Hz, 3H), 2.74 (s, 3H), 3.83 (q, J = 5.5 Hz, 1H), 7.50 (dd, J = 2.5, 8.5 Hz, 1H), 7.63 (dd, J = 2, 8.5 Hz, 1H), 7.83 (s, 2H), 7.98 (dd, J = 2.5, 8.5 Hz, 1H), 8.16 (s, 1H); ^{13}C NMR (150.9 MHz, DMSO-d_6) 18.81, 43.50, 45.28, 120.83, 123.79, 126.45, 127.86, 127.86, 129.29, 131.10, 133.11, 141.20, 143.96, 175.59; HRMS: *m/z* calcd for $C_{14}H_{14}O_3S$ $(M+H)^+$ 263.0736; found 263.0741.

2-(6-(Methylsulfonyl)naphthalen-2-yl)propanoic acid, 11. 2-(6-(Methylthio)naphthalen-2-yl)propanoic acid **9** (82.5 mg, 0.33 mmol) was dissolved in 10 mL of acetone:water (2:1). To this solution was added Oxone (445.5 mg, 0.73 mmol) which was allowed to stir at room temperature for 2 hours. The reaction mixture was extracted with ethyl ether (3x), dried over $MgSO_4$, and concentrated *in vacuo* to give pure product **11** (56 mg, yield 60 %, purity 97.8%, HPLC retention time 8.78 min, melting

point 180-182 °C). ^{1}H NMR (600 MHz, DMSO-d_6) δ 1.45 (d, J = 6 Hz, 1H), 3.24 (s, 3H), 3.92 (q, J = 5.5 Hz, 1H), 7.61 (dd, J = 2.5, 8.5 Hz, 1H), 7.91 (dd, J = 2.5, 8.5 Hz, 1H), 7.94 (s, 1H), 8.13-8.14 (m, 2H), 8.51 (s, 1H); ^{13}C NMR (150.9 MHz, DMSO-d_6) 18.75, 44.05, 45.37, 122.93, 126.40, 128.34, 128.41, 129.78, 130.04, 131.16, 135.26, 138.16, 142.89, 175.44; HRMS: *m/z* calcd for $C_{14}H_{14}O_4S$ $(M+H)^+$ 279.0686; found 279.0926.

2-(6-Methoxynaphthalen-2-yl)butanoic acid, 14. To a flask charged with 18 mL of THF and purged with argon was added magnesium ribbon (435.6 mg, 18 mmol) and a crystal of iodine. To this solution was added 2-bromo-6-methoxynapthalene (3.6 g, 15 mmol) in 18 mL of THF. An off brown color appeared, and the reaction was allowed to reflux for 1 hour. The reaction was then allowed to cool, and methyl 2- bromobutyrate (5.4 g, 3.4 mL, 30.2 mmol) was added. Following 2 hours of reflux, the reaction was quenched with 1M HCl, then extracted with ethyl ether (3x), washed with brine, dried with $MgSO_4$ and concentrated under reduced pressure. The crude mixture was suspended in 18 mL of a 3M KOH solution in MeOH, held at reflux for 2 hours, cooled, and then quenched with water. The reaction mixture was extracted with ethyl ether (3x). The aqueous layer was then acidified with 1 M HCl, extracted into ethyl ether (3x), washed with brine, dried with $MgSO_4$, and concentrated under reduced pressure to give crude product **14.** The product was purified using HPLC on a C18 column (2 g, yield 55%, purity 99.8%, HPLC retention time 15.8 min, melting point 115-117 °C) to give pure racemic product. ^{1}H NMR (600 MHz, DMSO-d_6) δ □0.84 (t, J = 7 Hz, 3H), 1.74-1.77 (m, 1H), 2.02-2.06 (m, 1H), 3.52 (t, J = 5.5 Hz, 1H), 3.86 (s, 3H), 7.11 (dd, J = 2.5, 8.7

Hz, 1H), 7.28 (d, *J* = 2.5 Hz, 1H), 7.40 (dd, *J* = 2.5, 8.7 Hz, 1H), 7.71 (s, 1H), 7.76-7.80 (m, 2H); ^{13}C NMR (150.9 MHz, DMSO-d_6) 12.56, 26.50, 53.01, 55.63, 106.17, 119.16, 126.69, 126.99, 127.31, 128.86, 129.57, 133.78, 135.24, 157.56, 175.40; HRMS: *m/z* calcd for $C_{15}H_{16}O_3$ $(M-H)^-$ 243.1027; found 243.1024.

2-(6-Methoxynaphthalen-2-yl)-*N*-(methylsulfonyl)butanamide, 15. To an ice-cold mixture (0-5 °C) of 2-(6-methoxynaphthalen-2-yl)butanoic acid **14.** [42] (87 mg, 0.39 mmol) in dry CH_2Cl_2 (3 mL) under argon was added 1,1′-carbonyldiimidazole (63 mg, 0.39 mmol). After the reaction mixture was stirred for two hours at 0-5 °C, methanesulfonamide (33 mg, 0.39 mmol) and diazabicyclo[5.4.0]undec-7-ene (59 mg, 0.39 mmol) (1 equiv.) were added. The mixture was left stirring for another four hours at ambient temperature before it was quenched by the addition of glacial acetic acid (52 uL) and diluted with additional CH_2Cl_2 (1 mL). The organic layer was separated and washed with 10% NaH_2PO_4 buffer (pH 4) (2 x 3 mL) and water (3 x 3 mL), dried over Na_2SO_4, filtered, and concentrated under reduced pressure to give a crude residue. The raw product was purified by flash chromatography (SiO_2, ethyl acetate/hexane gradient) to afford the product (52 mg, yield 45%, purity 98.5%, HPLC retention time 11.20 min, melting point 144-146 ^{o}C) of the pure title compound. ^{1}H NMR (600 MHz, DMSO-d_6) δ 0.82 (t, *J* = 7.46 Hz, 3H), 1.73-1.75 (m, 1H), 2.02-2.06 (m, 1H), 3.18 (s, 3H), 3.61 (t, *J* = 7.04 Hz, 1H), 3.85 (s, 3H), 7.14 (dd, *J* = 9.5, 2.1 Hz, 1H), 7.27 (d, *J* = 2.2 Hz, 1H), 7.39 (dd, *J* = 9.2, 2.0 Hz, 1H), 7.69 (s, 1H), 7.77 (d, *J* = 9.7 Hz, 1H), 7.79 (d, *J* = 9.8 Hz, 1H); ^{13}C NMR (150.9 MHz, DMSO-d_6) 12.37, 26.37, 41.35, 53.35, 55.61, 106.14, 119.22, 126.78, 126.84, 127.38, 128.75, 129.62, 133.88, 134.24, 157.67, 173.72; HRMS: *m/z*

calcd for $C_{16}H_{19}NO_4S$ $(M-H)^-$ 320.0962; found 320.0966.

Determination of the configuration of naproxen enantiomers 9a, 9b and 14a and 14b.

The configuration of compounds was inferred by comparing the order of elution of the two enantiomers of compound 9 (**9a** and **9b**) and the two enantiomers of compound **14** (**14a** and **14b**) from chiral columns with the order of elution of naproxen (*S*-isomer) and *R*-naproxen from the same column. A mixture of *R*- and *S*-naproxen, *R*-naproxen, *S*-naproxen, compound **9**, **9a** and **9b** were resolved on a Chiral AD-RH column (150 x 4. 6mm) using an isocratic elution method with a mobile phase of 60% HPLC grade water: 40% acetonitrile containing 0.1% formic acid. By contrast a mixture of *R*- and *S*-naproxen, *R*-naproxen, *S*-naproxen, compound **14**, **14a** and **14b** were resolved on a ChiralPak 1C (150 x 4.6 mm) column using an isocratic elution method. The mobile phase was 0.05%TFA in Hexane: 0.05% TFA in EtOH (98.5% : 1.5%) with a flow rate of 1.0 ml/min at room temperature (see Supporting Information).

Ligand Alignment and Molecular Docking

The structural models of the ligand-enzyme interactions used in the ligand alignment and docking experiments are based on the existing crystal structures of AKR1C3•$NADP^+$ complexed with *R*-naproxen, AKR1C3•$NADP^+$ complexed with *S*-naproxen and AKR1C2•$NADP^+$ complexed with *S*-naproxen. In the first stage, *R*-naproxen was docked to the AKR1C2•$NADP^+$ structure to generate AKR1C2•$NADP^+$ complexed with *R*-naproxen since no crystal structure of this complex has been published. The second round

of molecular modeling aligned **14a** and **14b** to their template ligand-enzyme structures. The results were overlaid to compare differences in the binding interactions of naproxen analogs in AKR1C2 and AKR1C3. For complete details see Supporting Information.

Enzyme purification

Homogenous recombinant enzymes AKR1C1-4 were prepared and purified as previously described. [61] Enzymes were purified to constant specific activity and their purity established by SDS-PAGE, see Supporting Information. All AKR enzymes were stored at -80 ºC in 20 mM potassium phosphate buffer pH 7.0 containing 30% glycerol, 1 mM EDTA and 1 mM β-mercaptoethanol. Under standard assay conditions the specific activity of AKR1C1 for the NAD^+ dependent oxidation of 1-acenaphthenol (Sigma) was 2.0 μmol min^{-1} mg^{-1}. The specific activities of AKR1C2 and AKR1C3 for the NAD^+ dependent oxidation of *S*-tetralol (Sigma) were 1.5 and 2.0 μmol min^{-1} mg^{-1}, respectively; and the specific activity of AKR1C4 for the NAD^+ dependent oxidation of androsterone (Steraloids) was 0.3 μmol min^{-1} mg^{-1} and are in agreement with previously published values. The specific activities of AKR1C enzymes were determined by measuring the formation of NADH at 340 nm using a Beckman DU640 spectrophotometer. A typical assay solution contained 100 mM potassium phosphate pH 7.0, 2.3 mM NAD^+, 200 μM 1-acenaphthenol for AKR1C1, 3.0 mM *S*-tetralol for AKR1C2 and 1C3, 75 μM androsterone for AKR1C4, 4% acetonitrile (v/v). The mixtures were incubated at 25 ºC (AKR1C1 and 1C4) or 37 ºC (AKR1C2 and 1C3) for 3 min followed by adding a serial dilution of enzyme solution to a final volume of 1 mL to initiate the reaction. After continuously monitoring for 5 min, the increase in UV absorption using different

concentrations of enzyme were recorded to calculate the initial velocity of substrate oxidation and determine enzyme specific activity.

COX-1 was purified to homogeneity from ram seminal vesicles.[62] The purity of the enzyme was assessed by SDS-PAGE (see Supporting Information).. The specific activity of COX-1 for the conversion of arachidonic acid to prostaglandin H_2 (PGH_2) was coupled to the oxidation of *N*, *N*, *N', N'*-tetramethyl-1, 4-phenylenediamine (TMPD) and was found to be. 1.0 μmol min^{-1} mg^{-1}. The specific activity of COX-1 enzyme was determined by measuring the formation of oxidized TMPD at 610 nm using Synergy 2 plate reader (BioTek). A typical assay solution (200 μL) contained 100 mM Tris-HCl (pH 8.0), 2 μM Hemin (Sigma), 5% DMSO, a serial dilution of COX-1 enzyme solution, 80 μM TMPD (Sigma) and 20 μM arachidonic acid (Sigma). Reagents were mixed and incubated at 25 ^{o}C for 5 min followed by adding a mixture of TMPD and arachidonic acid to initiate the reaction. Specific activity was determined based on the initial velocity of the reduction of PGG_2 formed in the reaction.

Enzyme Assays

S-Tetralol oxidation assay: the inhibitory potency of an individual compound against the AKR1C isoforms was determined by monitoring the $NADP^+$ dependent oxidation of *S*-tetralol catalyzed by the AKR1C enzymes using Synergy 2 plate reader (BioTek). Reaction systems (200 μL) contained 100 mM potassium phosphate buffer (pH 7.0), 4% DMSO, 200 μM $NADP^+$, a serial dilution of compounds, *S*-tetralol and AKR1C enzymes. The concentration of *S*-tetralol used in the inhibition assays using AKR1C1,

1C2, 1C3 and 1C4 was 5 μM, 22.5 μM, 165 μM and 25 μM respectively, which was equal to their *Km* values in order to make a direct comparison of IC_{50} values. The concentration of AKR1C1, 1C2, 1C3 and 1C4 was 111 nM, 86 nM, 95 nM and 552 nM, respectively. Reagents were mixed and incubated at 37 ^{o}C for 10 min followed by adding AKR1C enzymes to initiate the reaction. A continuous fluorometric assay (Ex: 340 nm, Em: 460 mM) to measure NADPH formation was conducted at 37 ^{o}C for 5 min and the IC_{50} value of each compound was calculated as previously described. To determine the pattern of inhibition, five fixed concentrations of *S*-tetralol were used and four different concentrations of inhibitor were used. The equations for COMP, NONCOMP and UNCOMP were globally fit to the initial velocity data using Grafit 5.0.6.

Reduction of Ketosteroids by Radiochemistry: Compounds were tested for their ability to inhibit the AKR1C3 catalyzed, reduction of [^{3}H]-Δ^{4}–AD and the AKR1C2 catalyzed reduction of [^{3}H]-5α-DHT. Compounds were incubated with purified recombinant enzyme and radiolabeled steroid in 100 mM phosphate buffer pH7.0 and 4% DMSO at 37˚C. The reaction was initiated by the addition of 1 mM NADPH, aliquots were removed over time and subsequently quenched by the addition of ice cold ethyl acetate. The ethyl acetate fraction was extracted and dried *in vacuo*. Steroid reference standards and extracts were dissolved in 50 μl ethyl acetate and applied to LK6D Silica TLC plates (Whatman Inc., Clifton, NJ). TLC plates were developed using a dichloromethane/ethyl acetate (80:20 v/v) solution and were scanned with a Bioscan System 200 plate reader (Washington, DC). The percentage of radioactivity in the product peak was calculated assuming that the combined radioactivity in the substrate

and product peaks was 100%. Initial velocities were computed by converting the percentage of radioactivity in the product peak by the specific radioactivity of the starting material to generate pmoles/min. The pattern of AKR1C3 inhibition was determined using five fixed concentrations of [^{3}H]-Δ^4–AD using 5 concentrations of inhibitor. Equations for COMP, NONCOMP and UNCOMP were fitted to the initial velocity data as described above.

COX-1 Assay: The effect of the compounds on COX-1 activity were determined by monitoring the oxidation of TMPD when coupled to COX catalyzed formation of prostaglandin H_2 (PGH_2) from PGG_2 using arachidonic acid as substrate. In brief, 200 µL of reaction solution was composed of 100 mM Tris-HCl (pH 8.0), 2 µM Hemin (Sigma), 5% DMSO, a serial dilution of compounds, COX-1 enzyme (175 nM), 80 µM TMPD (Sigma) and 20 µM arachidonic acid (Sigma). Reagents were mixed and incubated at 25 ^oC for 5 min followed by adding a mixture of TMPD and arachidonic acid to initiate the reaction. A continuous colorimetric assay to measuring TMPD oxidation at 610 nm was conducted using Synergy 2 plate reader at 25 ^oC for 5 min and IC_{50} value of each compound was calculated as previously described.[37]

Cell-Based Assays

AR-Luciferase Assay- HeLa13 [63] cells stably expressing the AR and a luciferase reporter gene construct were used for this assay as previously described. [37,47] Briefly, cells were cultured in phenol red free media supplemented with 5% CDFBS (CSS media) for 48 h. The cells were then harvested and plated in a 96 well plate for 6-7 h after which fresh CSS media (see below) containing 1 nM 5α-DHT in the presence of inhibitor was

added. After 20 h incubation, the media was removed and the luciferase activity in the cells was measured using the Bright Glo kit (Promega) according to the manufacturer's instructions. Fold induction of luciferase was evaluated relative to untreated cells.

Western blots: LNCaP cells stably expressing AKR1C3 (LNCaP-AKR1C3 cells) [64] seeded at a density of 1.5 x 10^6 cells were plated in 6 cm dishes containing phenol red free RPMI-1640 media supplemented with 5% CDFBS, 1% Pen/Strep and 2 mM L-Glutamine (CSS media). The cells were incubated for 24 h after which media was aspirated and fresh CSS media containing 100 nM Δ^4–AD plus and minus inhibitors. The cells were incubated for 24 h after which they were harvested in RIPA lysis buffer supplemented with protease inhibitors at 4 ^oC. Lysate protein concentration was determined by the Bradford assay using the BIORAD protein dye (Bio-Rad). The samples were subjected to electrophoresis on a 12% SDS-PAGE gel that was subsequently transferred to a nitrocellulose membrane. The membrane was probed with the appropriate antibodies as follows; anti β–tubulin (Millipore, # 05-661) anti-PSA (Meridian Life Science, Inc., #K92110R). Blots were imaged using the ECL reagent (Pierce) and GelDoc XR+ System and Image Lab software (Bio-Rad).

Radiometric assay of androgen metabolism: LNCaP-AKR1C3 cells seeded at a density of 1.5 x 10^6 cells were plated in 6 well plates in CSS media. The cells were allowed to incubate for 24 h, after which the media was aspirated and fresh CSS media with 7.5 nM (1.26 μCi) of [^{3}H] **Δ**^{4}-AD and 92.5 nM of cold Δ^4-AD (to obtain a final concentration of 100 nM) was added in the presence and absence of 30 μM of compound **14a** in each well. The cells were incubated for 48 h, after which time the media was

collected for analysis as previously described [63]. The media was extracted twice with cold ethyl acetate. In order to determine radioactivity of each phase, a portion of each fraction was added to Ultima Gold (Perkin Elmer Life Sciences) scintillation fluid and analyzed on a TriCarb 2100 (Packard Instruments, Perkin Elmer Life Sciences), all CPM counts were blank-adjusted and reported as corrected cpm. The aqueous phases were acidified to pH 6.5 with acetic acid and subjected to treatment with 400 U of *E. coli* β-glucuronidase at 37°C for 24 h. The de-conjugated androgens were re-extracted as described above, dried *in vacuo* and re-dissolved in 100 µL ethyl acetate for separation on the multi-channel LK6D Silica TLC plates. Plates were developed using dichloromethane/ethyl acetate (80:20 v/v) and scanned on the BioScan 200 plate reader.

ASSOCIATED CONTENT

Supporting Information

Supporting information containing molecular formula strings, PDB files for molecular models, SDS-PAGE of homogeneous enzymes, and chiral separation of compounds 9a, 9b, 14a, and 14b are provided free of charge at: http://pubs.acs.org

AUTHOR INFORMATION

Corresponding Author: Phone: (215)-898-9445; email address: penning@upenn.edu (T.M. Penning).

Present/Current Author Addresses: Dr. Adegoke Adeniji, Department of Pharmaceutical Sciences, South University School of Pharmacy, 709 Mall Blvd, Savannah, GA 31406

Author Contributions- Dr. Adegoke Adeniji wrote the first draft of the manuscript and performed the initial screening experiments. Dr. Md Jashim Uddin synthesized the naproxen analogs. Dr. Indy Zang conducted additional screening experiments and chiral separation of enantiomers. Dr. Daniel Tamae performed the cell-based assays, and Dr. Phumvadee Wangtrakuldee performed the molecular modeling studies. Compounds were supplied or synthesized in the laboratory of Dr. Larry J. Marnett. Dr. Marnett edited drafts of the manuscript. Dr. Trevor Penning conceived of the study, directed all the work and edited the final manuscript.

Notes

A provisional patent application was filed for the compounds described on October 22, 2015 at the US patent office (US Provisional Patent Application No. 62/244,934).

Dr. Trevor Penning is founder of Penzymes and both Drs. Penning and Marnett have an equity share in the LLC.

ACKNOWLEGEMENTS

Supported by P01-CA163227 and P30-ES013508 from the NIH to TMP and by CA89450 and GM15431 to LJM. We are grateful to Andy Liedtke for synthesis and characterization of some of the early compounds.

ABBREVIATIONS USED

Δ4-AD, 4-androstene-3,17-dione, AA, abiraterone acetate; ADT, androgen deprivation therapy; AKR1C3, aldo-keto reductase 1C3; AR, androgen receptor; COX, cylcooxygenases (PGH_2-synthase I and II); CRPC, castration resistant prostate cancer; 5α-DHT, 5α-dihydrotestosterone; ENZ, enzalutamide; NSAID, nonsteroidal anit-inflammatory drug, PSA, prostate specific antigen; TLC, thin layer chromatography.

REFERENCES

(1) Knudsen, K. E.; Penning, T.M. Partners in crime: deregulation of AR activity and androgen synthesis in prostate cancer. *Trends Endocrinol. Metab.* **2010,** *21*, 315-324.

(2) Knudsen, K. E.; Scher, H.I. Starving the addiction: new opportunities for durable suppression of AR signaling in prostate cancer. *Clin. Cancer Res.* **2009,** *15*, 4792-4798.

(3) Locke, J. A.; Guns, E.S.; Lubik, A.A.; Adomat, H.H.; Hendy, S.C.; Wood, C.A.; Ettinger, S.L.; Gleave, M.E.; Nelson, C.C. Androgen levels increase by intratumoral *de novo* steroidogenesis during progression of castration-resistant prostate cancer. *Cancer Res.* **2008,** *68*, 6407-6415.

(4) Montgomery, R. B.; Mostaghel, E.A; Vessella, R.; Hess, D.L.; Kalhorn, T.F.; Higano, C.S.; True, L.D.; Nelson, P.S. Maintenance of intratumoral androgens in metastatic prostate cancer: a mechanism for castration-resistant tumor growth. *Cancer Res.* **2008,** *68*, 4447-4454.

(5) Mostaghel, E. A.; Page, S.T.; Lin, D.W.; Fazli, L.; Coleman, I.M.; True, L.D.; Knudsen, B.; Hess, D.L.; Nelson, C.C.; Matsumoto, A.M.; Bremner, W.J.; Gleave, M.E.; Nelson, P.S. Intraprostatic androgens and androgen-regulated gene expression persist after testosterone suppression: therapeutic implications for castration-resistant prostate cancer. *Cancer Res.* **2007,** *67*, 5033-5041.

(6) Visakorpi, T.; Hyytinen, E.; Koivisto, P.; Tanner, M.; Keinänen, R.; Palmberg, C.; Palotie, A.; Tammela, T.; Isola, J.; Kallioniemi, O.P. *In vivo* amplification of the androgen receptor gene and progression of human prostate cancer. *Nat. Genet.* **1995,** *9*, 401-406.

(7) Shi, X.-B.; Ma, A-H.; Xia, L.; Kung, H-J.; de Vere White, R. W. Mutational analysis of 44 mutant androgen receptors from human prostate cancer. *Cancer Res.* **2002,** *62*, 1496-1502.

(8) Taplin, M. E.; Bubley, G.J.; Shuster, T.D.; Frantz, M.E.; Spooner, A.E.; Ogata, G.K.; Keer, H.N.; Balk, S.P. Mutation of the androgen-receptor gene in metastatic androgen-independent prostate cancer. *N. Engl. J. Med.* **1995,** *332*, 1393-1398.

(9) Antonarakis, E. S.; Lu, C.; Wang, H.; Luber, B.; Nakazawa, M.; Roeser, J.C.; Chen, Y.; Mohammad, T.A.; Chen, Y.; Fedor, H.L.; Lotan, T.L.; Zheng, Q.; De Marzo, A.M.; Isaacs, J.T.; Isaacs, W.B.; Nadal, R.; Paller, C.J.; Denmeade, S.R.; Carducci, M.A.; Eisenberger, M.A.; Luo, J. AR-V7 and resistance to enzalutamide and abiraterone in prostate cancer. *N. Engl. J. Med.* **2014,** *371*, 1028-1038.

(10) Sprenger, C. C.; Plymate, S.R. The link between androgen receptor splice variants and castration-resistant prostate cancer. *Hormones & Cancer* **2014,** *5*, 207-2014.

(11) O'Donnell, A.; Judson, I.; Dowsett, M.; Raynaud, F.; Dearnaley, D.; Mason, M.; Harland, S.; Robbins, A.; Halbert, G.; Nutley, B.; Jarman, M. Hormonal impact of the 17α-hydroxylase/C(17,20)-lyase inhibitor abiraterone acetate (CB7630) in patients with prostate cancer,. *British Journal of Cancer* **2004,** *90*, 2317-2325.

(12) Attard, G.; Reid, A.H.; Yap, T.A.; Raynaud, F.; Dowsett, M.; Settatree, S.; Barrett, M.; Parker, C.; Martins, V.; Folkerd, E.; Clark, J.; Cooper, C.S.; Kaye, S.B.; Dearnaley, D.; Lee, G.; de Bono, J.S. Phase I clinical trial of a selective inhibitor of CYP17, abiraterone acetate, confirms that castration-resistant prostate cancer commonly remains hormone driven. *J. Clin. Oncol.* **2008,** *26*, 4563-4571.

(13) Attard, G.; Reid, A.H.; A'Hern, R.; Parker, C.; Oommen, N.B.; Folkerd, E.; Messiou, C.; Molife, L.R.; Maier, G.; Thompson, E.; Olmos, D.; Sinha, R.; Lee, G.; Dowsett, M.; Kaye, S.B.; Dearnaley, D.; Kheoh, T.; Molina, A.; de Bono, J.S. Selective inhibition of CYP17 with abiraterone acetate is highly active in the treatment of castration-resistant prostate cancer. *J. Clin. Oncol.* **2009,** *27*, 3742-3748.

(14) Reid, A. H.; Attard, G.; Danila, D.C.; Oommen, N.B.; Olmos, D.; Fong, P.C.; Molife, L.R.; Hunt, J.; Messiou, C.; Parker, C.; Dearnaley, D.; Swennenhuis, J.F.; Terstappen, L.W.; Lee, G.; Kheoh, T.; Molina, A.; Ryan, C.J.; Small, E.; Scher, H.I.; de Bono, J.S. Significant and sustained antitumor activity in post-docetaxel, castration-resistant prostate cancer with the CYP17 inhibitor abiraterone acetate. *J. Clin. Oncol.* **2010,** *28*, 1489-1495.

(15) de Bono, J. S.; Logothetis, C.J.; Molina, A.; Fizazi, K.; North, S.; Chu, L.; Chi, K.N.; Jones, R.J.; Goodman, Jr. O. B.; Saad, F.; Staffurth, J.N.; Mainwaring, P.;

Harland, S.; Flaig, T.W.; Hutson, T.E.; Cheng, T.; Patterson, H.; Hainsworth, J.D.; Ryan, C.J.; Sternberg, C.N.; Ellard, S.L.; Flechon, A.; Saleh, M.; Scholz, M.; Efstathiou, E.; Zivi, A.; Bianchini, D.; Loriot, Y.; Chieffo, N.; Kheoh, T.; Haqq, C.M.; Scher, H.I. Abiraterone and increased survival in metastatic prostate cancer. *N. Engl. J. Med.,* **2011,** *364*, 1995-2005.

(16) Cai, C.; Chen, S.; Ng, P.; Bubley, G.J.; Nelson, P.S.; Mostaghel, E.A.; Marck, B.; Matsumoto, A.M.; Simon, N.I.; Wang, H.; Balk, S.P. Intratumoral *de novo* steroid synthesis activates androgen receptor in castration-resistant prostate cancer and is upregulated by treatment with CYP17A1 inhibitors. *Cancer Res.* **2011,** *71*, 6503-6513.

(17) Mostaghel, E. A.; Marck, B.T.; Plymate, S.R.; Vessella, R.L.; Balk, S.P.; Matsumoto, A.M.; Nelson, P.S; Montgomery, R.B. Resistance to CYP17A1 inhibition with abiraterone in castration-resistant prostate cancer: induction of steroidogenesis and androgen receptor splice variants. *Clin. Cancer Res.* **2011,** *17*, 5913-5925.

(18) Lin, H.-K; Jez, J.M.; Schlegel, B.P.; Peehl, D.M.; Pachter, J.A.; Penning, T.M. Expression and characterization of recombinant type 2 3α-hydroxysteroid dehydrogenase (HSD) from human prostate: demonstration of bifunctional 3α/17β-HSD activity and cellular distribution. *Mol. Endocrinol.* **1997,** *11*, 1971-1984.

(19) Penning, T. M.; Burczynski, M.E.; Jez, J.M.; Hung, C.F.; Lin, H.K.; Ma, H.; Moore, M.; Palackal, N.; Ratnam, K. Human 3α-hydroxysteroid dehydrogenase isoforms (AKR1C1-AKR1C4) of the aldo-keto reductase superfamily: functional plasticity and tissue distribution reveals roles in the inactivation and formation of male and female sex hormones;. *Biochem. J.* **2000,** *351*, 67-77.

(20) Mohler, J. L.; Titus, M.A.; Bai, S.; Kennerley, B.J.; Lih, F.B.; Tomer, K.B.; Wilson, E.M. Activation of the androgen receptor by intratumoral bioconversion of androstanediol to dihydrotestosterone in prostate cancer. *Cancer Res.* **2011,** *71*, 1486-1496.

(21) Auchus, R. J. The backdoor pathway to dihydrotestosterone. *Trends Endocrinol. Metab.* **2004,** *15*, 432-438.

(22) Fung, K.-M.; Shea-Samara, E.H.; Wong, C.; Krin, R.; Jones, A.M.; Bane, B.; Liu, C.Z.; Yang, J.T.; Pitha, J.V.; Culkin, D.J.; Koop, B.P.; Penning, T.M.; Lin, H-K. Increased expression of type 2 3α-hydroxysteroid dehydrogenase/type 5 17β-hydroxysteroid dehydrogenase (AKR1C3) and its relationship with the androgen receptor in prostate carcinoma. *Endocr. Related Cancer* **2006,** *13*, 169-180.

(23) Mitsiades, N.; Sung, C. C.; Schultz, N.; Danila, D. C.; He, B.; Eedunuri, V. K.; Fleisher, M.; Sander, C.; Sawyers, C. L.; Scher, H. I. Distinct patterns of dysregulated expression of enzymes involved in androgen synthesis and metabolism in metastatic prostate cancer tumors. *Cancer Res.* **2012,** *72*, 6142-6152.

(24) Hamid, A.H.; Pfeiffer, M.I.; Verhaegh, G.W.; Schaafsma, E.; Brandt, A.; Sweep, F. C.; Sedelaar, J.P.; Schalken, J.A. Aldo-keto reductase 1 member C3 (AKR1C3) is a biomarker and therapeutic target for castration-resistant prostate cancer. *Mol. Med.* **2012,** *18*, 1449-1455.

(25) Stanbrough, M.; Bubley, G.J.; Ross, K.; Golub, T.R.; Rubin, M.A.; Penning, T.M.; Febbo, P.G.; Balk, S.P. Increased expression of genes converting adrenal

androgens to testosterone in androgen-independent prostate cancer. *Cancer Res.* **2006,** *66*, 2815-2825.

(26) Tian, Y.; Zhao, L.; Zhang, H.; Liu, X.; Zhao, L.; Zhao, X.; Li, J. AKR1C3 overexpression may serve as a promising biomarker for prostate cancer progression. *Diagnostic Pathol.* **2014,** *9*, 42-48.

(27) Hofland, J.; van Weerden, W.M.; Dits, N.F.; Steenbergen, J.; van Leenders, G.J.; Jenster, G.; Schroder, F.H.; de Jong, F.H. Evidence of limited contributions for intratumoral steroidogenesis in prostate cancer. *Cancer Res.* **2010,** *70*, 1256-1264.

(28) Pfeiffer, M. J.; Smit, F. P.; Sedelaar, J. P.; Schalken, J. A. Steroidogenic enzymes and stem cell markers are upregulated during androgen deprivation in prostate cancer. *Mol Med.* **2011,** *17*, 657-664.

(29) Powell, K.; Semann, L.; Conley-LaComb, M.K.; Asangani, I.; Wu, Y-M.; Ginsburg, K.B.; Williams, J.; Squire, J.A.; Maddipati, K.R.; Cher, M.L.; Chinni, S.R. ERG/AKR1C3/AR constitutes a feed-forward loop for AR signaling in prostate cancer cells. *Clin. Cancer Res.* **2015,** *21*, 2569-2579.

(30) Yepuru, M.; Wu, Z.; Kulkarni, A.; Yin, F.; Barrett, C.M.; Kim, J.; Steiner, M.S.; Miller, D.D.; Dalton, J.T.; Narayanan, R. Steroidogenic enzyme AKR1C3 is a novel androgen receptor-selective coactivator that promotes prostate cancer growth. *Clin. Cancer Res.* **2013,** *19*, 5613-5625.

(31) Beer, T. M.; Armstrong, A.J.; Rathkopf, D.E.; Loroit, Y.; Sternberg, C.N.; Higano, C.S.; Iverson, P.; Bhattacharya, S.; Carles, J.; Chowdury, S.; Davis, I.D.; de Bono, J.S.; Evans, C.P.; Fizazi, K.; Joshua, A.M.; Kim, C-S.; Kimura, G.; Mainwairng,

P.; Mansbach, H.; Miller, K.; Nonnberg, S.B.; Perabo, F.; Phung, D.; Sadd, F.; Scher, H.I.; Taplin, M-E.; Venner, P.M.; Tombal, B. for the PREVAIL Investigators. Enzalutamide in metastatic prostate cancer before chemotherapy. *N. Engl. J. Med.* **2014,** *371*, 424-433.

(32) Scher, H. I.; Beer, T.M.; Higano, C.S.; Anand, A.; Taplin, M.E.; Efstathiou, E.; Rathkopf, D.; Shelkey, J.; Yu, E.Y.; Alumkal, J.; Hung, D.; Hirmand, M.; Seely, L.; Morris, M.J.; Danila, D.C.; Humm, J.; Larson, S.; Fleisher, M.; Sawyers, C.L. Prostate Cancer Foundation/Department of Defense Prostate Cancer Clinical Trials Consortium. antitumour activity of MDV3100 in castration-resistant prostate cancer: a phase 1-2 study. *Lancet* **2010,** *375*, 1437-1446.

(33) Tran, C.; Ouk, S.; Clegg, N.J.; Chen, Y.; Watson, P.A.; Arora, V.; Wongvipat, J.; Smith-Jones, P.M; Yoo, D.; Kwon, A.; Wasielewska, T.; Welsbie, D.; Chen, C.D.; Higano, C.S.; Beer, T.M.; Hung, D.T.; Scher, H.I.; Jung, M.E.; Sawyers, C.L. Development of a second-generation antiandrogen for treatment of advanced prostate cancer. *Science.* **2009**, *324*, 787-790.

(34) Byrns, M. V.; Steckelbroeck, S.; Penning, T.M. An indomethacin analogue, N-(4-chlorobenzoyl)-melatonin, is a selective inhibitor of aldo-keto reductase 1C3 (type 2 3α-HSD, type 5 17β-HSD, and prostaglandin F synthase), a potential target for the treatment of hormone dependent and hormone independent malignancies. *Biochem. Pharmacol.* **2008,** *75*, 484-493.

(35) Liu, C.; Lou, W.; Zhu, Y.; Yang, J.C.; Natiminty, N.; Gaikwad, N.; Evans, C.P.; Gao, A.C. Intracrine androgens and AKR1C3 activation confer resistance to enzalutamide in prostate cancer. *Cancer Res.* **2015,** 75, 1413-1422

(36) Adeniji, A. O.; Twenter, B.M.; Byrns, M.C.; Jin, Y.; Chen, M.; Winkler, J.D.; Penning, T.M. Development of potent and selective inhibitors of aldo-keto reductase 1C3 (type 5 17β-hydroxysteroid dehydrogenase) based on *N*-phenyl-aminobenzoates and their structure-activity relationships. *J. Med. Chem.* **2012,** *55*, 2311-2323.

(37) Liedtke, A. J.; Adeniji, A.O.; Chen, M.; Byrns, M.C.; Jin, Y.; Christianson, D.W.; Marnett, L.J.; Penning, T.M. Development of potent and selective indomethacin analogues for the inhibition of AKR1C3 (type 5 17β-hydroxysteroid dehydrogenase/prostaglandin F synthase) in castrate-resistant prostate cancer. *J. Med. Chem.* **2013,** *56*, 2429-2446.

(38) Rizner, T. L.; Lin, H.K.; Peehl, D.M.; Steckelbroeck, S.; Bauman, D.R.; Penning, T.M. Human type 3 3α-hydroxysteroid dehydrogenase (aldo-keto reductase 1C2) and androgen metabolism in prostate cells. *Endocrinology* **2003,** *144*, 2922-2932.

(39) Steckelbroeck, S.; Jin, Y.; Gopishetty, S.; Oyesanmi, B.; Penning, T.M. Human cytosolic 3α-hydroxysteroid dehydrogenases of the aldo-keto reductase superfamily display significant 3β-hydroxysteroid dehydrogenase activity: implications for steroid hormone metabolism and action. *J. Biol. Chem.* **2004,** *279*, 10784-10795.

(40) Penning, T. M.; Bauman, D.R.; Jin, Y.; Rizner, T.L. Identification of the molecular switch that regulates access of 5α-DHT to the androgen receptor. *Mol. Cell. Endocrinol.* **2007,** *265-266*, 77-82.

(41) Gu, Y.; Guise, C.P.; Patel, K.; Abbattista, M.R.; Li, J.; Sun, X.; Atwell, G.J.; Boyd, M.; Patterson, A.V.; Wilson, W.R. Reductive metabolism of the dinitrobenzamide mustard anticancer prodrug PR-104 in mice,. *Cancer Chemother. Pharmacol.* **2011,** *67*, 543-555.

(42) Duggan, K. C.; Walters, M.J.; Musee, J.; Harp, J.M.; Kiefer, J.R.; Oates, J.A.; Marnett, L.J. Molecular basis for cyclooxygenase inhibition by the non-steroidal anti-inflammatory drug naproxen. *J. Biol. Chem.* **2010,** *285*, 34950-34959.

(43) Duggan, K. C.; Hermanson, D.J.; Musee, J.; Prosakiewicz, J.J.; Scheib, J.L.; Carter, B.D.; Banerjee, S.; Oates, J.A.; Marnett, L.J. (*R*)-Profens are substrate-selective inhibitors of endocannabinoid oxygenation by COX-2. *Nat. Chem. Biol.* **2011,** 803-809.

(44) Byrns, M. C.; Jin, Y.; Penning, T.M. Inhibitors of type 5 17β-hydroxysteroid dehydrogenase (AKR1C3): overview and structural insights. *J. Steroid. Biochem. & Mol. Biol.* **2011,** *125*, 95-104.

(45) Byrns, M. C.; Penning, T.M. Type 5 17β-hydroxysteroid dehydrogenase/prostaglandin F synthase (AKR1C3): role in breast cancer and inhibition by non-steroidal anti-inflammatory drug analogs,. *Chemico-Biol. Inter.* **2009,** *178*, 221-227.

(46) Adeniji, A. O.; Chen, M.; Penning, T.M. AKR1C3 as a target in castrate resistant prostate cancer, *J. Steroid. Biochem. & Mol. Biol.* **2013,** *137*, 136-149.

(47) Chen, M.; Adeniji, A.O.; Twenter, B.M.; Winkler, J.D.; Christianson, D.W.; Penning, T.M. Crystal structures of AKR1C3 containing an *N*-(aryl)amino-benzoate

inhibitor and a bifunctional AKR1C3 inhibitor and androgen receptor antagonist. *Bioorg. & Med. Chem. Letts.,* **2012,** *22*, 3492-3497.

(48) Flanagan, J. U.; Yosaatmadja, Y.; Teague, R.M.; Chai, M.Z.; Turnbull, A.P.; Squire, C.J. Crystal structures of three classes of non-steroidal anti-inflammatory drugs in complex with aldo-keto reductase 1C3 . *PLoS One* **2012,** e43965.

(49) Gazvoda, M.; Beranic, N.; Turk, S.; Burja, B.; Kocevar, M.; Rizner, T.J.; Gobec, S.; Polanc, S. 2,3-Diarylpropenoic acids as selective non-steroidal inhibitors of type-5 17β-hydroxysteroid dehydrogenase (AKR1C3). *Eur. J. Med. Chem.* **2013,** *62*, 89-97.

(50) Heinrich, D. M.; Flanagan, J.U.; Jamieson, S.M.; Silva, S.; Rigoreau, L.J.; Trivier, E., Raynham, T.; Turnbull, A.P.; Denny, W.A. Synthesis and structure-activity relationships for 1-(4-(piperidin-1-ylsulfonyl)phenyl)pyrrolidin-2-ones as novel non-carboxylate inhibitors of the aldo-keto reductase enzyme AKR1C3. *Eur. J. Med. Chem.* **2013,** *62*, 738-744.

(51) Kikuchi, A.; Furutani, T.; Azami, H.; Watanbe, K.; Nimi, T.; Kamiyama, Y.; Kuromitsu, S.; Bakin-Bey, E.; Heeringa, M.; Uoatas, T.; Enjo, K. *In vitro* and *in vivo* characterization of ASP9521: a novel selective, orally bioavailable inhibitor of 17β-hydroxysteroid dehydrogenase type 5 (17β-HSD5; AKR1C3). *Invest. New Drugs* **2014,** *32*, 860-870.

(52) Skarydova, L.; Hofman, J.; Chlebek, J.; Havrankova, J.; Kosanova, K.; Skarka, A.; Hostalkova, A.; Plucha, T.; Cahlikova, L.; Wsol, V. Isoquinoline alkaloids as a novel type of AKR1C3 inhibitors . *J. Steroid. Biochem. & Mol. Biol.* **2014,** *143C*, 250-258.

(53) Adeniji, A.; Twenter, B.M.; Byrns, M.C.; Jin, Y.; Winkler, J.D.; Penning, T.M. Discovery of substituted 3-(phenylamino)benzoic acids as potent and selective inhibitors of type 5 17β-hydroxysteroid dehydrogenase (AKR1C3). *Bioorg. & Med. Chem. Letts,* **2011,** *21*, 1464-1468.

(54) Harrison, I. T.; Lewis, B.; Nelson, P.; Rooks, W.; Roszkowski, A.; Tomolonis, A.; Fried, J.H. Nonsteroidal antiinflammatory agents. I. 6-substituted 2-naphthylacetic acids. *J. Med. Chem.* **1970,** *13*, 203-205.

(55) Bauman, D. R.; Rudnick, S.I.; Szewczuk, L.M.; Jin, Y.; Gopishetty, S., Penning, T.M. Development of nonsteroidal anti-inflammatory drug analogs and steroid carboxylates selective for human aldo-keto reductase isoforms: potential antineoplastic agents that work independently of cyclooxygenase isozymes. *Mol. Pharmacol.* **2005,** *67*, 60-68.

(56) Jackson, V. J.; Yosaatmadja, Y.; Flanagan, J.U.; Squire, C.J. Structure of AKR1C3 with 3-phenoxybenzoic acid bound,. *Acta Crystallogr Sect F Struct Biol Cryst Commun,* **2012,** *68*, 409-413.

(57) Lovering, A. L.; Ride, J.P.; Bunce, C.M.; Desmond, J.C.; Cummings, S.M.; White, S.A. Crystal structures of prostaglandin D(2) 11-ketoreductase (AKR1C3) in complex with the nonsteroidal anti-inflammatory drugs flufenamic acid and indomethacin. *Cancer Res.* **2004,** *64*, 1802-1810.

(58) Gant, T. G.; Sarshar, S.; Woo, H. Preparation and utility of substituted carboxylic acid compounds as COX-modulators. *USA Patent* **2007,** US20070276042A1; 20071129.

(59) Arewang, C. J; Lahmann, M.; Oscarson, S.; Tiden, A. Synthesis of urine drug metabolites: glucuronic and glycosides of phenol intermediates. *Carbohyd. Res.* **2007,** *342*, 970-974.

(60) Kovacs, I.; Belanger-Gariepy, F.; Shaver, A. Synthesis and characterization of mononuclear iron silanethiolato complexes containing an un supported Fe-Si-Si bond system: X-ray structure of CpFe(CO)2SSiPh$_3$ and its reaction with SO_2. *Inorg. Chem.* **2003,** *42*, 2988-2991.

(61) Burczynski, M. E.; Harvey, R.G., Penning, T.M. Expression and characterization of four recombinant human dihydrodiol dehydrogenase isoforms: oxidation of *trans*-7, 8-dihydroxy-7,8-dihydrobenzo[*a*]pyrene to the activated o-quinone metabolite benzo[*a*]pyrene-7,8-dione. *Biochemistry* **1998,** *37*, 6781-6790.

(62) Smith, T.; Leipprandt, J.; DeWitt, D. Purification and characterization of the human recombinant histidine-tagged prostaglandin endoperoxide H synthases-1 and -2. *Arch. Biochem. Biophys.,* **2000,** *375*, 195-200.

(63) Cherian, M. T.; Wilson, E.M.; Shapiro, D.J. A competitive inhibitor that reduces recruitment of androgen receptor to androgen-responsive genes,. *J. Biol. Chem.* **2012,** *287*, 23368-23380.

(64) Byrns, M. C.; Mindnich, R.; Duan, L.; Penning, T.M. Overexpression of aldo-keto reductase 1C3 (AKR1C3) in LNCaP cells diverts androgen metabolism towards testosterone resulting in resistance to the 5α-reductase inhibitor finasteride. *J. Steroid. Biochem. & Mol. Biol.* **2012,** *130*, 7-15.

Table of Contents Graphic

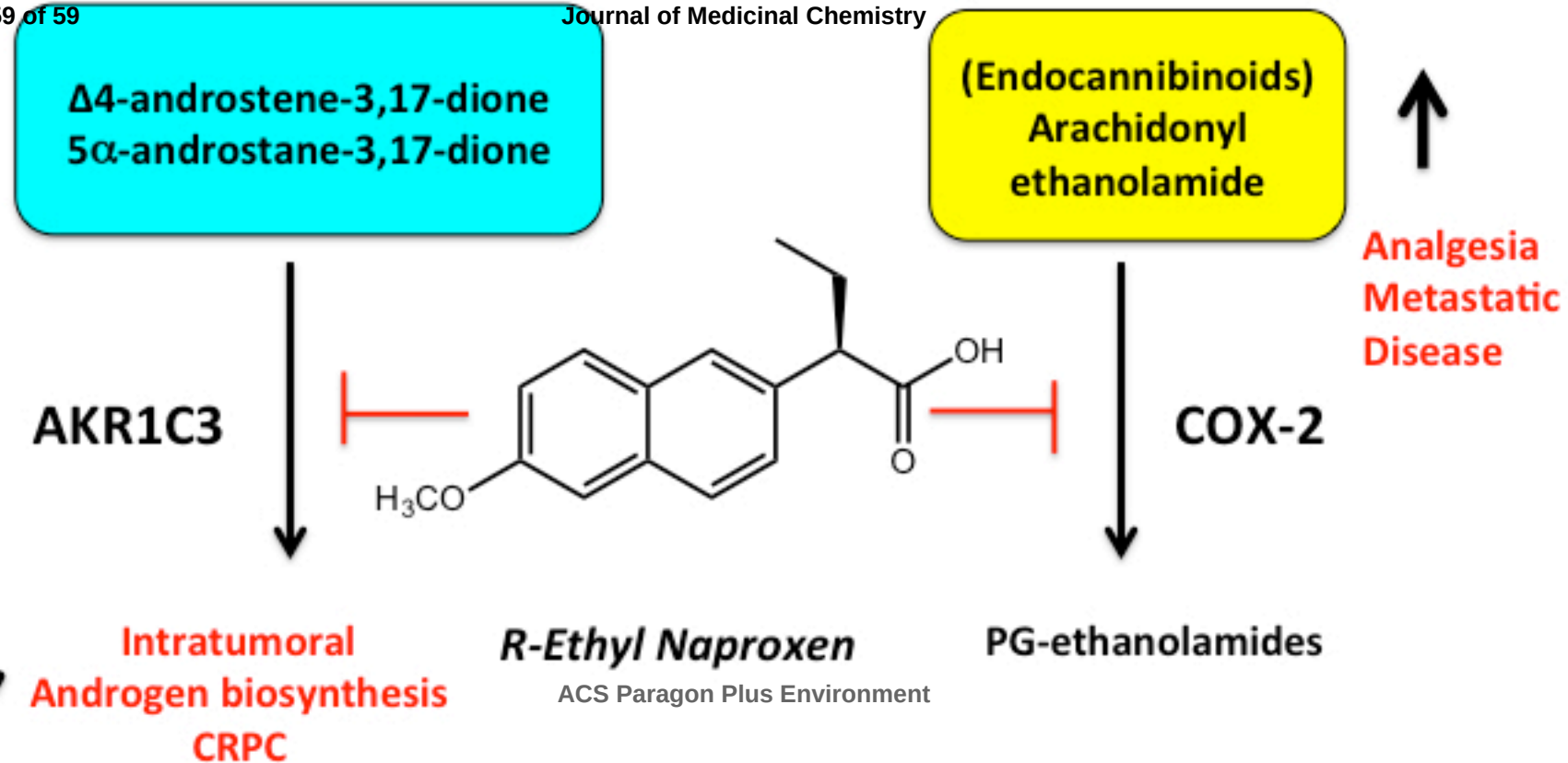
Δ4-androstene-3,17-dione
5α-androstane-3,17-dione
(Endocannibinoids)
Arachidonyl
ethanolamide
Analgesia
Metastatic
Disease
AKR1C3
COX-2
OH
O
H3CO
Intratumoral
Androgen biosynthesis
CRPC
R-Ethyl Naproxen
PG-ethanolamides